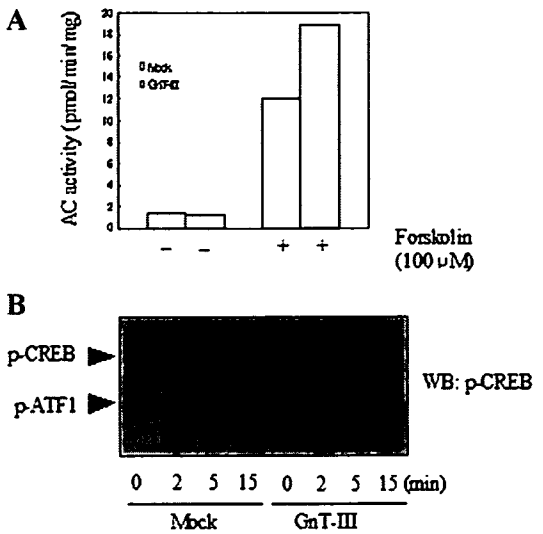

Fig. 2. Forskolin-induced AC activation and CREB phosphorylation are enhanced in GnT-III-transfected B16 cells. (**A**) AC assay of B16 cells. For each reaction, 10 μg membrane fractions were prepared, treated with or without 100 μM forskolin at 30 °C for 20 min, and AC activity was determined as described in the *Materials and methods* section. The figure shows one representative experiment of three independent experiments. (**B**) After serum starvation for 16 h, B16 cells were treated with 10 μM forskolin for 0, 2, 5, and 15 min. The cell lysates were subjected to 10% SDS–PAGE and western blotting was performed using a specific anti-phospho-CREB antibody. Phosphorylated ATF1 (p-ATF1), a protein related to CREB, can also be detected by the anti-phospho-CREB antibody.

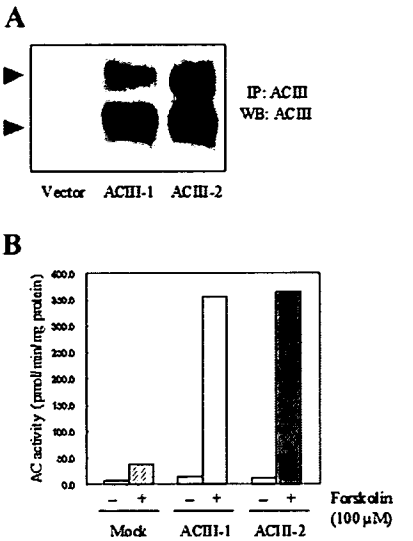

Fig. 4. Establishment of Flp-In 293 cells stably expressing ACIII. (**A**) Cell lysates of ACIII transfectants were immunoprecipitated with an anti-ACIII antibody, and the immunoprecipitated ACIII was subjected to 8% SDS–PAGE. Western blotting was performed by using an anti-ACIII antibody. The pcDNA5/FRT transfectant was used as a control. (**B**) AC assay was performed for ACIII stable expression cell lines. For each reaction, 10 μg of membrane fractions was prepared, treated with or without 100 μM forskolin at 30 °C for 20 min, and AC activity was determined as described in the *Materials and methods* section. pcDNA5/FRT transfectant was used as a control. The figure shows one representative experiment of three independent experiments.

293 cells. The expression levels of ACIII were confirmed by both western blotting and an activity assay. The ACIII transfectants showed two bands by immunoprecipitation and western blotting using an ACIII antibody, and the molecular masses were about 180 and 120 kDa (Figure 4A), consistent with previously reported data (Wei et al. 1996). As evidenced by the forskolin-treatment, AC activity was about 10 times higher enzymatic compared with the control (Figure 4B). These results indicate that ACIII stable expression cell lines were successfully established.

The profile of ACIII in GnT-III-transfected Flp-In 293 cells stably expressing ACIII

GnT-III, the D323A dominant negative mutant of GnT-III, and vector were then transfected into Flp-In 293 cells stably

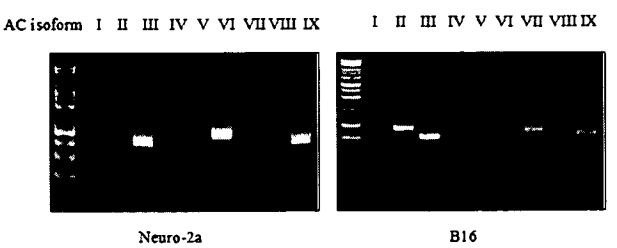

Fig. 3. Identification of endogenous AC isoforms in Neuro-2a and B16 cells by RT–PCR. mRNA expression of endogenous AC isoforms was examined by RT–PCR. Total RNA was isolated from Neuro-2a and B16 cells and reverse transcriptase reactions were performed. The cDNAs were amplified by PCR as described in the *Materials and methods* section. The specific primers used are listed in Table I.

expressing ACIII, and the effect of GnT-III was investigated. The expression levels of GnT-III were confirmed by western blotting using a GnT-III-specific antibody and a GnT-III activity assay (data not shown). A western blot revealed that the protein levels of ACIII in each transfectant were similar (Figure 5A, left panel). When a lectin blot was performed, E_4-PHA reacted with the upper band of ACIII in the GnT-III transfectants but not with ACIII in the mock transfectant and D323A dominant negative mutant of GnT-III transfectant (Figure 5A, right panel), indicating that *N*-glycans of ACIII in the GnT-III transfectant were modified by the insertion of a bisecting GlcNAc. When the cells were treated with *N*-glycosidase F (PNGase F), which cleaves *N*-glycans between the innermost *N*-acetylglucosamine and asparagines residue, only the lower bands could be detected (Figure 5B), indicating that the upper bands represented the glycosylated form and the lower bands represented the non-glycosylated form, as was suggested in a previous report (Wei et al. 1996). We confirmed that the cell surface expression levels of ACIII in the GnT-III transfectants and mock transfected or D323A dominant negative mutant of GnT-III-transfected cells were nearly the same (Figure 5C), but only the upper bands of the ACIII were detected.

Forskolin-induced ACIII activity is increased in GnT-III-transfected Flp-In 293 cells stably expressing ACIII

AC activity in the GnT-III transfectants was examined. When cells were treated with 100 μM forskolin, the GnT-III transfectants showed an increased AC activity compared with mock transfectants and the D323A dominant negative mutant of GnT-III transfectants, as expected (Figure 6). Furthermore, when cells were treated with PMA, a calmodulin-dependent

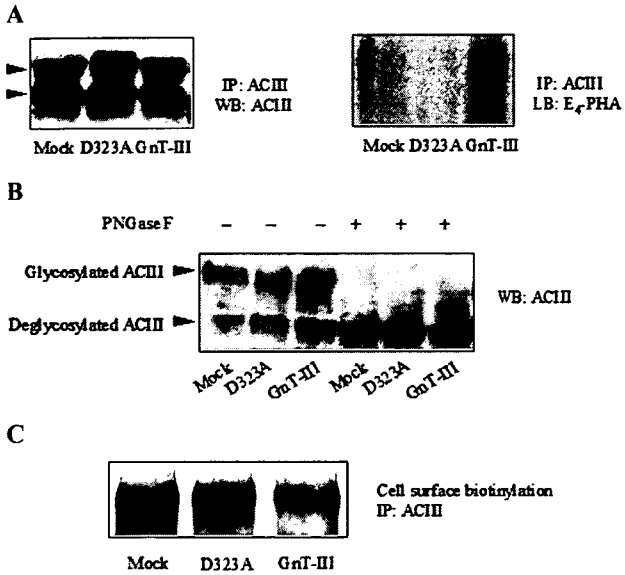

Fig. 5. The profile of in GnT-III-transfected Flp-In-293 cells ACIII stably expressing ACIII. (**A**) GnT-III, D323A dominant negative mutant of GnT-III, and vector were transfected into Flp-in 293 cells stably expressing ACIII. Cell lysates were immunoprecipitated with an anti-ACIII antibody, and the immunoprecipitated ACIII was subjected to 8% SDS–PAGE. Western blotting was performed using an anti-ACIII antibody (left panel) and with E_4-PHA (right panel). (**B**) Membrane fractions were prepared and treated with PNGase F as described in the *Materials and methods* section. The samples were subjected to 8% SDS–PAGE and analyzed by western blotting using an anti-ACIII antibody. (**C**) Cell surface expression of ACIII in co-overexpression cells of ACIII and GnT-III. The cell surfaces of the transfectants were biotinylated by treatment with sulfo-NHS-Biotin at room temperature for 30 min, and ACIII was immunoprecipitated using an anti-ACIII antibody. The samples were subjected to 8% SDS–PAGE and transferred to a PVDF membrane. After blocking in 3% bovine serum albumin (BSA) overnight, biotinylated bands were detected with an ABC kit and an ECL kit.

kinase II inhibitor, or a phosphodiesterase E inhibitor, AC activity in the GnT-III transfectants was slightly increased, but the difference compared with control cells was not significant (data not shown), indicating that GnT-III transfection specifically affects the forskolin-ACIII pathway.

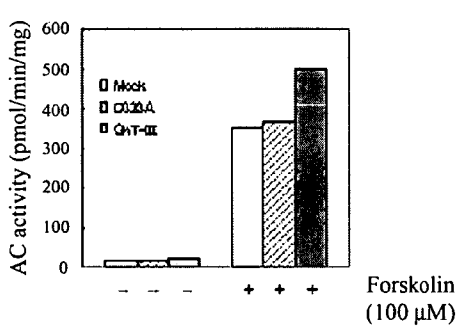

Fig. 6. Forskolin-induced AC activity is increased in GnT-III-transfected Flp-In-293 cells stably expressing ACIII. AC assay was performed in Flp-In-293 cells stably expressing ACIII transfected with GnT-III, D323A dominant negative mutant of GnT-III, or vector. For each reaction, 10 μg membrane fractions were prepared, treated with or without 100 μM forskolin at 30 °C for 20 min, and AC activity was determined as described in the *Materials and methods* section. The pcDNA5/FRT transfectant was used as a control. The figure shows one representative experiment of three independent experiments.

Discussion

AC isoforms are tightly controlled by various signals and therefore contribute to the complexity of cellular signaling mechanisms. ACIII is expressed in several tissues including brain, spinal cord, adrenal medulla, adrenal cortex, heart atrium, aorta, lung, retina (Xia et al. 1992), testis and spermatozoa (Defer et al. 1998; Gautier-Courteille et al. 1998; Livera et al. 2005), but it is particularly abundant in olfactory tissue, where it may play a major role in coupling olfactory receptors to cAMP and ion channel regulation (Bakalyar and Reed 1990). It has been demonstrated that ACIII-deficient mice fail several olfaction-based behavioral tests and lack electro-olfactogram responses elicited by either cAMP or inositol triphosphate, despite the presence of other AC isoforms in the olfactory cilia (Wong et al. 2000). In these knockout mice, ACIII has also been implicated as an important mediator of prostaglandin E_2-induced growth inhibition in arterial smooth muscle cells (Wong et al. 2001). Point mutations in the promoter region of the ACIII-encoding gene associated with the restoration of insulin release by forskolin have been reported in a type 2 diabetes model rat (Abdel-Halim et al. 1998). Thus, ACIII is possibly involved in various crucial biological events.

In this study, we reported that glycosyltransferase GnT-III participates in the regulation of the AC signaling pathway. We found that the overexpression of GnT-III up-regulates AC activity in Neuro-2a mouse neuroblastoma cells and B16 mouse melanoma cells (Figures 1B and 2A). In those GnT-III transfectants, downstream signaling such as the formation of cellular cAMP and CREB phosphorylation, is also enhanced (Figures 1A, C and 2B). To elucidate the mechanism by which AC activity is enhanced in the GnT-III transfectants, we constructed a stable expression system of ACIII and GnT-III using Flp-In 293 cells. We confirmed that neither the total expression nor the cell surface expression levels of ACIII were changed in the GnT-III transfectants (Figure 5A and C). Experiments with PNGase F suggest that ACIII is glycosylated in Flp-In 293 cells, and that the upper band represents the glycosylated form and the lower band the unglycosylated form (Figure 5B). The results of lectin blotting indicated that *N*-glycan of the upper band of ACIII is modified by the insertion of a bisecting GlcNAc in the GnT-III transfectants (Figure 5A). It appears likely that the modification of *N*-glycan affects the function of ACIII itself, since activity was measured in the membrane fraction preparations, which might be free from AC-regulating molecules (Figure 6), although we cannot completely rule out the possibility that the addition of bisecting GlcNAc to other glycoproteins in addition to ACIII affects AC activity.

The function of the *N*-glycan of ACs has been studied by several groups; it was proposed that glycosylation is involved in the Ca^{2+}-induced phosphorylation of ACIII (Wei et al. 1996). The glycosylation of ACVI significantly affects its catalytic activity in an activator-dependent manner and also alters the sensitivity of ACVI to the inhibition induced by a Gαi-coupled receptor or by PKC (Wu et al. 2001). The glycosylation state of ACVIII affects the catalytic activity without altering its K_m values or its dependence on calmodulin (Cali et al. 1996). These results strongly suggest that the *N*-glycan on ACs regulates AC activity. In the present study, we examined the effects of the modification of *N*-glycan structure of ACIII.

We assume that other AC isoforms might also be involved in the up-regulation of forskolin-induced CREB phosphorylation in GnT-III. The detailed-mechanisms of how bisecting GlcNAc affects ACIII activity remain to be elucidated, but the possibility that ACIII with a bisecting GlcNAc becomes less responsive to inhibitory signals cannot be excluded since *N*-glycans regulate protein–protein interactions. In the case of ACVI, sensitivity toward the Gαi-coupled dopamine D2 receptor decreases by the deletion of glycans. Since GnT-III is a key enzyme that inhibits the extension and modification of *N*-glycans by introducing a bisecting GlcNAc, it is possible that GnT-III transfection reduces the interaction between certain residues of the *N*-glycan of ACIII and inhibitory molecules.

Previous studies have shown that GnT-III affects a number of intracellular signaling pathways (Yoshimura et al. 1996; Ihara et al. 1997; Kitada et al. 2001; Sato et al. 2001; Bhattacharyya et al. 2002; Shibukawa et al. 2003; Yang et al. 2003; Zhao et al. 2006). For example, when GnT-III is overexpressed in PC12 cells, Trk A, a nerve growth factor receptor, is modified with a bisecting GlcNAc, which suppresses its dimerization (Ihara et al. 1997). GnT-III overexpression in HeLaS3 cells leads to the up-regulation of endocytosis of epidermal growth factor receptor (Sato et al. 2001). Furthermore, GnT-III transfection in HeLaS3 cells suppressed H_2O_2-induced activation of the PKCδ–JNK1 pathway, resulting in the inhibition of apoptosis (Shibukawa et al. 2003). Since cAMP is involved in a variety of physiological activities, the up-regulation of AC activity in GnT-III transfectants might be involved in the mechanisms of the above-observed phenomena.

Our results suggest that *N*-glycans on ACIII play an important role in regulating its activity. In a future study, we plan to analyze the structures of AC-linked *N*-glycans and to conduct detailed studies of the mechanisms by which *N*-glycans affect AC function.

Materials and methods

Promoter–reporter assay

To determine the pathway that is up-regulated in the GnT-III transfectants, we utilized the Pathway Profiling Systems (Clontech, Palo Alto, CA). Briefly, Neuro-2a cells were plated in six-well plates and transfected with promoter–reporter plasmids using Lipofectamine 2000 as described in the manufacturer's protocol. These plasmids contained the luciferase reporter gene downstream of several copies of specific transcription factor-binding sequences such as AP-1, CRE, HSE, Myc, and NF-κB. After incubation at 37 °C for 18 h, the cells were starved for 7 h and then treated with different chemicals. Cells were lysed and luciferase activities were measured using the Dual-Luciferase Reporter Assay (Promega, Madison, WI) following the manufacturer's protocol.

Construction of GnT-III and ACIII expression vectors

Rat GnT-III was subcloned in pCXN2 (Niwa et al. 1991), which contains a neo gene, and is regulated by the β-actin promoter. A D323A dominant negative mutant of GnT-III was constructed as reported previously. D323 in GnT-III is supposed to be involved in the coordination of a divalent cation such as Mn^{2+} along with a phosphoryl group of the donor nucleotide sugar and thus crucial for the enzymatic activity (Ihara et al. 2002). Human ACIII cDNA was cloned from human brain RNA; the full-length of human ACIII was amplified by RT–PCR with the following primers: CAGCAACATG TCATGGTTTAG (sense); CTTCAGCTGAATTTGTGGCTG (antisense). The coding region of ACIII was subcloned into a eukaryotic expression vector, pcDNA5/FRT (Invitrogen, Carlsbad, CA), driven by the cytomegalovirus promoter, for a stable high expression Flp-In system.

Cell culture and transfection

Neruo-2a mouse neuroblastoma cells and B16 mouse melanoma cells were maintained in Dulbecco's modified Eagle's medium (DMEM, low glucose), and Flp-In 293 cells (Invitrogen) were maintained in DMEM (high glucose) supplemented with 10% fetal bovine serum in an incubation chamber supplied with 5% CO_2 at 37 °C. The cells were transfected with the desired construct using Lipofectamine 2000 (Invitrogen) following the manufacture's protocol. For GnT-III transfection, cells were selected by treatment with 1000 μg/mL of neomycin for 2 weeks, and for ACIII transfection, the cells were selected by treatment with 200 μg/mL of hygromycin B (Calbiochem, La Jolla, CA) for 2 weeks. Antibiotic-resistant colonies were isolated and recloned by serial dilution to ensure clonality. To confirm the expression of GnT-III or ACIII, western blotting and an enzyme activity assay were performed.

Immunoprecipitation and western blotting

Cell cultures were washed with ice-cold phosphate-buffered saline (PBS) and harvested in lysis buffer [20 mM Tris–HCl, pH 7.4, 150 mM NaCl, 5 mM EDTA, 1% (w/v) Nonidet P-40, 10% (w/v) glycerol, 5 mM sodium pyrophosphate, 10 mM NaF, 1 mM sodium orthovanadate, 10 mM β-glycerophosphate, 1 mM phenylmethylsulfonyl fluoride (PMSF), 2 μg/mL aprotinin, 5 μg/mL leupeptin, and 1 mM dithiothreitol]. Cell lysates were centrifuged at 15 000 rpm for 15 min to obtain supernatants, and protein concentrations were determined using a protein assay CBB kit (Nacalai Tesque, Kyoto, Japan). For immunoprecipitation with ACIII, the lysate was incubated with a rabbit polyclonal antibody against ACIII (C-20) (Santa Cruz Biotechnology, Santa Cruz, CA) for 3 h at 4 °C and then with 15 μL of protein G-Sepharose for 2 h at 4 °C. For western blotting, whole cell lysates or immunoprecipitates were subjected to SDS polyacrylamide gel electrophoresis (PAGE), and transferred to a PVDF membrane (Amersham Pharmacia Biotech, Piscataway, NJ). The membrane was blocked with 5% (w/v) skimmed milk in Tris-buffered saline containing 0.1% (v/v) Tween-20 (TBST, pH 7.5) for 2 h at room temperature and incubated with antibodies against CREB (Cell signaling), phospho-CREB (Cell signaling), ACIII (C-20) (Santa Cruz) or GnT-III (Fuji rebio Inc., Tokyo, Japan) overnight at 4 °C. After washing with TBST, the membranes were treated with the second antibodies for 1 h at room temperature. The membranes were washed and immunoreactive bands were visualized using an ECL kit (Amersham Pharmacia), according to the manufacturer's instructions.

Measurement of total cellular cAMP

Cells were cultured overnight until 80% confluent in 96-well dishes (10^3 to 10^5 cells/well). After treatment with the indicated chemicals at 37 °C for 20 min, the cells were lysed and total cellular cAMP levels were determined using a Biotrak cAMP enzyme immunoassay kit (Amersham Pharmacia), following the manufacture's protocol.

Membrane fraction preparation for AC activity assay

Cells were harvested, resuspended in buffer A (25 mM Tris–HCl, 0.4 mM EDTA, 1 mM EGTA, 250 mM sucrose, 0.1 mM leupeptin, and 40 μM PMSF, pH 7.4), and homogenized using a glass Dounce homogenizer. The homogenate was centrifuged at 1500 rpm for 5 min to remove nuclei and broken cell pieces, and the supernatant centrifuged again at 50 000*g* for 30 min to collect the membrane fractions. The pelleted membrane fraction was resuspended in buffer B (10 mM Tris–HCl, pH 7.4, 10 mM EDTA, 5 mM $MgCl_2$), and the protein concentrations determined using a protein assay CBB kit (Nacalai Tesuque, Japan).

AC activity assay

The catalytic activities of AC were measured as described previously, with minor modifications (Onda et al. 2001). The reaction mixtures contained 20 mM HEPES (pH 8.0), 0.5 mM EDTA, 0.1 mM ATP containing [α-^{32}P] ATP (1×10^6 cpm) (Amersham Pharmacia), 0.1 mM cAMP, 1 mM creatine phosphate, 8 U/mL creatine phosphokinase, 5 mM $MgCl_2$, and 10 μg of membrane protein in a final volume of 100 μL. Reactions were performed at 30 °C for 20 min in the presence or absence of 100 μM forskolin and terminated by adding 10 μL of ice-cold 2.2 M HCl. The [^{32}P] cAMP produced was separated on acidic alumina columns (Alvarez and Daniels 1992). Briefly, the samples were applied to an acidic alumina column (ICN Pharmaceuticals, Inc., Costa Mesa, CA), which was washed with 5 mM HCl to remove any unbound contaminants, and the bound cAMP was eluted with 6 mL of 0.1 M ammonium acetate (pH 7.0). The radioactivity of the eluted samples was determined by scintillation counting.

RT–PCR analysis

Total RNA was prepared from Neuro-2a and B16 cells using the TRIzol reagent (Invitrogen), and the cDNAs were synthesized by Superscriptase II (Gibco BRL, Gaithersburg, MD) with an oligo (dT) primer. To determine the expression of each AC isoform, PCR was performed with the specific primers listed in Table I. The reaction conditions were as follows; 30 cycles of denaturation at 94 °C for 30 s, annealing at 60 °C for 30 s, and extension at 72 °C for 30 s. Amplified cDNA fragments were confirmed by DNA electrophoresis on 1% agarose gel.

Lectin blotting

The immunoprecipitated ACIII was electrophoresed on 8% SDS–PAGE and transferred to PVDF membranes, as described above. The membrane was blocked with 3% bovine serum albumin (BSA) (w/v) in TBST and then incubated with 1 μg/mL of biotinylated erythroagglutinating phytohemagglutinin (E_4-PHA) (Seikagaku Corp., Tokyo, Japan) in TBST for 30 min at room temperature. After washing with TBST for three times, lectin-reactive proteins were detected by using a Vectastain ABC kit (Vector Laboratories, Burlingame, CA) and an ECL kit.

PNGase F digestion

Whole-cell lysates of human ACIII transfectants were boiled with 0.1 M 2-mercaptoethanol and 0.1% SDS for 10 min. After boiling, the cell lysates were incubated with 60 mM Tris–HCl (pH 8.6), 0.8% Nonidet P-40, and 40 mU/mL of PNGase F (Roche Applied Science, Indianapolis, IN) at 37 °C, 16 h. The samples were then subjected to western blotting using an anti-ACIII antibody, as described above.

Cell surface biotinylation

Cells were cultured overnight until 80% confluence was reached. After washing three times with PBS supplemented with 0.1 mM $CaCl_2$ and 1 mM $MgCl_2$, the cells were incubated with 200 μg/mL of EZ-Link™ Sulfo-NHS-Biotin (Pierce, Rockford, IL) at room temperature for 30 min. The reaction was quenched with 25 mM Tris (pH 8.0) containing 150 mM NaCl. After washing three times with PBS, the cells were solubilized with 1 mL of lysis buffer, and the cell lysates were centrifuged at 15 000 rpm for 15 min to obtain the supernatant. Immunoprecipitation was performed using an anti-ACIII antibody and the immunoprecipitates were separated by 8% SDS–PAGE and then transferred to a PVDF membrane as described above. After blocking the membrane

Table I. Primers used in the RT–PCR of AC isoforms

Isomer	Sense	Antisense
ACI	ATGACGACAAGCGGAGGGCATT	CAAGGATGTAGGAAGTAGTCAGCC
ACII	AGACAACCCTTCCGACTGCCAAT	GACGCCAGCTATTACAGGTCCA
ACIII	CTGAGCTTTTACTACTTCTCGCGC	GAAGCCGTACTCTCGAAGGATGA
ACIV	CTGCTCCCTTTTTCTGCACATGAG	TTTGCCTTTGACCTTGATGCTGCC
ACV	ACGACGAAGACCCTCCACTAAG	ATAAAGTTCCTACGGGGCACCATC
ACVI	ACTTGGTGCTGCTTTTGCTGGG	AGTAGGTGGTCATCTCCCCCTT
ACVII	CTGAGACCAACGGGACACAAAG	CTGGAGGATAGTGCATGTCTCTTC
ACVIII	CTTAACTCTGTCCTGAAGCTGGCA	TGCCAAGTTCACAGTTTTCCCCCAA
ACIX	ATCCAGAGCATGAGAGACCAGG	CGAATACTGAACGGAAGGCACCAA

with 3% (w/v) BSA in TBST overnight, a Vectastain ABC kit and an ECL kit were used to detect the biotinylated protein.

Acknowledgments

Grant support was provided by the 21st Century COE Program from the Japan Society for the promotion of Science; Core Research for Evolutional Science and Technology from Japan Science and Technology Agency; and Special Coordination Funds for Promoting Science and Technology, the Ministry of Education, Culture, Sports, Science and Technology, Japan.

Conflict of interest statement

None declared.

Abbreviations

AC, adenylyl cyclase; ACIII, adenylyl cyclase type III; BSA, bovine serum albumin; CRE, cAMP response element; CREB, CRE-binding protein; DMEM, Dulbecco's modified Eagle's medium; GlcNAC, *N*-acetylglucosamine; GnT-III, β1, 4-*N*-acetylglucosaminyltransferase III; HSE, heat shock element; PAGE, polyacrylamide gel electrophoresis; PBS, phosphate-buffered saline; PKA, cAMP-dependent protein kinase A; PKC, protein kinase C; PMSF, phenylmethylsulfonyl fluoride; PNGase, *N*-glycosidase F; TBST, Tris-buffered saline with Tween-20.

References

Abdel-Halim SM, Guenifi A, He B, Yang B, Mustafa M, Hojeberg B, Hillert J, Bakhiet M, Efendic S. 1998. Mutations in the promoter of adenylyl cyclase (AC)-III gene, overexpression of AC-III mRNA, and enhanced cAMP generation in islets from the spontaneously diabetic GK rat model of type 2 diabetes. Diabetes. 47:498–504.

Alvarez R, Daniels DV. 1992. A separation method for the assay of adenylyl-cyclase, intracellular cyclic AMP, and cyclic-AMP phosphodiesterase using tritium-labeled substrates. Anal Biochem. 203:76–82.

Bakalyar HA, Reed RR. 1990. Identification of a specialized adenylyl cyclase that may mediate odorant detection. Science. 250:1403–1406.

Bhattacharyya R, Bhaumik M, Raju TS, Stanley P. 2002. Truncated, inactive *N*-acetylglucosaminyltransferase III (GlcNAc-TIII) induces neurological and other traits absent in mice that lack GlcNAc-TIII. J Biol Chem. 277: 26300–26309.

Cali JJ, Parekh RS, Krupinski J. 1996. Splice variants of type VIII adenylyl cyclase. Differences in glycosylation and regulation by Ca2+/calmodulin. J Biol Chem. 271:1089–1095.

Defer N, Marinx O, Poyard M, Lienard MO, Jegou B, Hanoune J. 1998. The olfactory adenylyl cyclase type 3 is expressed in male germ cells. FEBS Lett. 424:216–220.

Dennis JW, Granovsky M, Warren CE. 1999. Glycoprotein glycosylation and cancer progression. Biochim Biophys Acta. 1473:21–34.

Freeze HH, Aebi M. 2005. Altered glycan structures: the molecular basis of congenital disorders of glycosylation. Curr Opin Struct Biol. 15:490–498.

Gautier-Courteille C, Salanova M, Conti M. 1998. The olfactory adenylyl cyclase III is expressed in rat germ cells during spermiogenesis. Endocrinology. 139:2588–2599.

Gu J, Nishikawa A, Tsuruoka N, Ohno M, Yamaguchi N, Kangawa K, Taniguchi N. 1993. Purification and characterization of UDP-*N*-acetylglucosamine: alpha-6-D-mannoside beta 1-6*N*-acetylglucosaminyltransferase (*N*-acetylglucosaminyltransferase V) from a human lung cancer cell line. J Biochem (Tokyo). 113:614–619.

Helenius A, Aebi M. 2004. Roles of N-linked glycans in the endoplasmic reticulum. Annu Rev Biochem. 73:1019–1049.

Ihara H, Ikeda Y, Koyota S, Endo T, Honke K, Taniguchi N. 2002. A catalytically inactive beta 1,4-*N*-acetylglucosaminyltransferase III (GnT-III) behaves as a dominant negative GnT-III inhibitor. Eur J Biochem. 269: 193–201.

Ihara Y, Sakamoto Y, Mihara M, Shimizu K, Taniguchi N. 1997. Overexpression of *N*-acetylglucosaminyltransferase III disrupts the tyrosine phosphorylation of Trk with resultant signaling dysfunction in PC12 cells treated with nerve growth factor. J Biol Chem. 272:9629–9634.

Kitada T, Miyoshi E, Noda K, Higashiyama S, Ihara H, Matsuura N, Hayashi N, Kawata S, Matsuzawa Y, Taniguchi N. 2001. The addition of bisecting *N*-acetylglucosamine residues to E-cadherin down-regulates the tyrosine phosphorylation of beta-catenin. J Biol Chem. 276:475–480.

Livera G, Xie F, Garcia MA, Jaiswal B, Chen J, Law E, Storm DR, Conti M. 2005. Inactivation of the mouse adenylyl cyclase 3 gene disrupts male fertility and spermatozoan function. Mol Endocrinol. 19:1277–1290.

Narasimhan S. 1982. Control of glycoprotein synthesis. UDP-GlcNAc:glycopeptide beta 4-*N*-acetylglucosaminyltransferase III, an enzyme in hen oviduct which adds GlcNAc in beta 1-4 linkage to the beta-linked mannose of the trimannosyl core of *N*-glycosyl oligosaccharides. J Biol Chem. 257:10235–10242.

Nishikawa A, Ihara Y, Hatakeyama M, Kangawa K, Taniguchi N. 1992. Purification, cDNA cloning, and expression of UDP-*N*-acetylglucosamine: beta-D-mannoside beta-1,4*N*-acetylglucosaminyltransferase III from rat kidney. J Biol Chem. 267:18199–18204.

Niwa H, Yamamura K, Miyazaki J. 1991. Efficient selection for high-expression transfectants with a novel eukaryotic vector. Gene. 108: 193–199.

Ohtsubo K, Takamatsu S, Minowa MT, Yoshida A, Takeuchi M, Marth JD. 2005. Dietary and genetic control of glucose transporter 2 glycosylation promotes insulin secretion in suppressing diabetes. Cell. 123:1307–1321.

Onda T, Hashimoto Y, Nagai M, Kuramochi H, Saito S, Yamazaki H, Toya Y, Sakai I, Homcy CJ, Nishikawa K et al. 2001. Type-specific regulation of adenylyl cyclase. Selective pharmacological stimulation and inhibition of adenylyl cyclase isoforms. J Biol Chem. 276:47785–47793.

Partridge EA, Le Roy C, Di Guglielmo GM, Pawling J, Cheung P, Granovsky M, Nabi IR, Wrana JL, Dennis JW. 2004. Regulation of cytokine receptors by Golgi *N*-glycan processing and endocytosis. Science. 306:120–124.

Premont RT, Matsuoka I, Mattei MG, Pouille Y, Defer N, Hanoune J. 1996. Identification and characterization of a widely expressed form of adenylyl cyclase. J Biol Chem. 271:13900–13907.

Rudd PM, Elliott T, Cresswell P, Wilson IA, Dwek RA. 2001. Glycosylation and the immune system. Science. 291:2370–2376.

Sato Y, Takahashi M, Shibukawa Y, Jain SK, Hamaoka R, Miyagawa J, Yaginuma Y, Honke K, Ishikawa M, Taniguchi N. 2001. Overexpression of *N*-acetylglucosaminyltransferase III enhances the epidermal growth factor-induced phosphorylation of ERK in HeLaS3 cells by up-regulation of the internalization rate of the receptors. J Biol Chem. 276:11956–11962.

Schachter H. 1986. Biosynthetic controls that determine the branching and microheterogeneity of protein-bound oligosaccharides. Biochem Cell Biol. 64:163–181.

Shibukawa Y, Takahashi M, Laffont I, Honke K, Taniguchi N. 2003. Down-regulation of hydrogen peroxide-induced PKC delta activation in *N*-acetylglucosaminyltransferase III-transfected HeLaS3 cells. J Biol Chem. 278: 3197–3203.

Smit MJ, Iyengar R. 1998. Mammalian adenylyl cyclases. Adv Second Messenger Phosphoprotein Res. 32:1–21.

Stanley P. 2002. Biological consequences of overexpressing or eliminating *N*-acetylglucosaminyltransferase-TIII in the mouse. Biochim Biophys Acta. 1573:363–368.

Sunahara RK, Dessauer CW, Gilman AG. 1996. Complexity and diversity of mammalian adenylyl cyclases. Annu Rev Pharmacol Toxicol. 36: 461–480.

Sunahara RK, Taussig R. 2002. Isoforms of mammalian adenylyl cyclase: multiplicities of signaling. Mol Interv. 2:168–184.

Tang WJ, Hurley JH. 1998. Catalytic mechanism and regulation of mammalian adenylyl cyclases. Mol Pharmacol. 54:231–240.

Taniguchi N, Miyoshi E, Jianguo G, Honke K, Matsumoto A. 2006. Decoding sugar functions by identifying target glycoproteins. Curr Opin Struct Biol. 16:561–566.

Taniguchi N, Miyoshi E, Ko JH, Ikeda Y, Ihara Y. 1999. Implication of *N*-acetylglucosaminyltransferases III and V in cancer: gene regulation and signaling mechanism. Biochim Biophys Acta. 1455:287–300.

Wei J, Wayman G, Storm DR. 1996. Phosphorylation and inhibition of type III adenylyl cyclase by calmodulin-dependent protein kinase II in vivo. J Biol Chem. 271:24231–24235.

Wong ST, Baker LP, Trinh K, Hetman M, Suzuki LA, Storm DR, Bomfeldt KE. 2001. Adenylyl cyclase 3 mediates prostaglandin E(2)-induced growth inhibition in arterial smooth muscle cells. J Biol Chem. 276: 34206–34212.

Wong ST, Trinh K, Hacker B, Chan GC, Lowe G, Gaggar A, Xia Z, Gold GH, Storm DR. 2000. Disruption of the type III adenylyl cyclase gene leads to peripheral and behavioral anosmia in transgenic mice. Neuron. 27: 487–497.

Wu GC, Lai HL, Lin YW, Chu YT, Chern Y. 2001. *N*-glycosylation and residues Asn805 and Asn890 are involved in the functional properties of type VI adenylyl cyclase. J Biol Chem. 276:35450–35457.

Xia Z, Choi EJ, Wang F, Storm DR. 1992. The type III calcium/calmodulin-sensitive adenylyl cyclase is not specific to olfactory sensory neurons. Neurosci Lett. 144:169–173.

Yang X, Tang J, Rogler CE, Stanley P. 2003. Reduced hepatocyte proliferation is the basis of retarded liver tumor progression and liver regeneration in mice lacking *N*-acetylglucosaminyltransferase III. Cancer Res. 63: 7753–7759.

Yoshimura M, Ihara Y, Matsuzawa Y, Taniguchi N. 1996. Aberrant glycosylation of E-cadherin enhances cell-cell binding to suppress metastasis. J Biol Chem. 271:13811–13815.

Zhao Y, Nakagawa T, Itoh S, Inamori K, Isaji T, Kariya Y, Kondo A, Miyoshi E, Miyazaki K, Kawasaki N et al. 2006. *N*-acetylglucosaminyltransferase III antagonizes the effect of *N*-acetylglucosaminyltransferase V on alpha3-beta1 integrin-mediated cell migration. J Biol Chem. 281:32122–32130.

Inhalation Toxicology. 20:349–359, 2008

ISSN: 0895-8378 print / 1091-7691 online
DOI: 10.1080/08958370701866412

informa
healthcare

Decreased Airway Expression of Vascular Endothelial Growth Factor in Cigarette Smoke-Induced Emphysema in Mice and COPD Patients

Masaru Suzuki, Tomoko Betsuyaku, Katsura Nagai, Satoshi Fuke, and Yasuyuki Nasuhara
First Department of Medicine, Hokkaido University School of Medicine, Sapporo, Japan

Kichizo Kaga and Satoshi Kondo
Department of Surgical Oncology, Hokkaido University Graduate School of Medicine, Sapporo

Ichiro Hamamura, Junko Hata, and Hiroshi Takahashi
Teijin Institute for Bio-Medical Research, Teijin Pharma Ltd., Tokyo, Japan

Masaharu Nishimura
First Department of Medicine, Hokkaido University School of Medicine, Sapporo, Japan

Vascular endothelial growth factor (VEGF) signaling is crucial for lung structure maintenance. Although VEGF deficiency plays a role in the pathogenesis of emphysema in animals, little is known about VEGF expression levels and functions, as well as VEGF receptors, in airway epithelial cells, which are in direct contact with the environment. In this study, C57BL/6J mice were exposed to cigarette smoke (CS) for short (~10 days) and long (4–24 wk) time periods, and bronchiolar expressions of VEGF and its receptors VEGFR-1 and VEGFR-2 were examined. The relationships between the expressions of VEGF, VEGFR-1, and VEGFR-2 and smoking histories and/or chronic obstructive pulmonary disease (COPD) were examined in humans. The mRNA levels were quantified in bronchiolar epithelium harvested by laser capture microdissection in both mouse and human lung tissues or in human bronchial epithelium harvested by bronchoscopic brushing. The VEGF protein level was assessed by immunohistochemistry or enzyme-linked immunosorbent assay. Repeated CS exposure downregulated bronchiolar expressions of VEGF and both VEGF receptors at various time points prior to the development of emphysema. In humans, bronchiolar VEGF was significantly decreased in smokers with COPD compared to lifelong nonsmokers, as well as to smokers without COPD; however, there was no difference in bronchiolar VEGF levels between lifelong nonsmokers and smokers without COPD. On the other hand, bronchiolar VEGFR-2 was downregulated in smokers with and without COPD compared to lifelong nonsmokers. These findings suggest the association of downregulation of bronchiolar VEGF and its receptors with cigarette smoking and COPD.

Chronic obstructive pulmonary disease (COPD) is characterized by airflow limitation that is not fully reversible; pulmonary emphysema is an important phenotype of COPD, characterized by destruction and enlargement of the pulmonary alveoli (Pauwels et al., 2001). COPD is a major public health problem, since it is the fifth leading cause of death worldwide, and its prevalence is expected to increase in the upcoming decades (Pauwels et al., 2004). Cigarette smoke (CS) is the major risk factor for COPD. However, the molecular and cellular mechanisms that are responsible for the development of COPD and/or emphysema are not fully understood.

Vascular endothelial growth factor (VEGF) is produced by many different cell types. It is thought to be important for maintaining structural homeostasis in the adult lung (Berse et al., 1992; Voelkel et al., 2006). VEGF binds to VEGF receptors VEGFR-1 and VEGFR-2 (Waltenberger et al., 1994; Ferrara et al., 2003). Recently, based on the results of several animal studies, VEGF has been implicated in the pathogenesis of

Received 3 September 2007; accepted 18 October 2007.
The authors thank Dr. Robert M. Senior of the Washington University School of Medicine for his helpful comments, Yoko Suzuki for her invaluable technical assistance in performing LCM and immunohistochemistry techniques, and Naomi Matsui and Yoshie Suzuki for their care and analysis of the mouse CS model.
Address correspondence to Tomoko Betsuyaku, MD, PhD, First Department of Medicine, Hokkaido University School of Medicine, North 15, West 7, Kita-ku, Sapporo, 060-8638, Japan. E-mail: bytomoko@med.hokudai.ac.jp

pulmonary emphysema (Kasahara et al., 2000; Tang et al., 2004; Marwick et al., 2006). We and others have recently reported that, even in the absence of lung disease, VEGF levels were decreased in bronchoalveolar lavage fluids obtained from healthy current smokers (Koyama et al., 2002a; Nagai et al., 2005). Decreased VEGF levels have been found in the sputum and whole lung tissues obtained from emphysema patients; however, these human studies lacked healthy smokers as controls (Kanazawa et al., 2003; Kasahara et al., 2001). We were the first to report that VEGF and VEGFR-1 expressions in alveolar macrophages were downregulated in older current smokers, even if they only had mild emphysema, compared to age-matched current smokers without emphysema (Nagai et al., 2005).

Due to their direct contact with the environment, epithelial cells located along the respiratory tract are particularly exposed to CS; therefore, they are likely to be involved in the pathogenesis of smoking-related diseases. The presence of VEGF, VEGFR-1, and VEGFR-2 in airway epithelium has been documented using immunohistochemistry (Fehrenbach et al., 1999; Kranenburg et al., 2005). Acute exposure to CS extract has been reported to upregulate VEGF mRNA in a human bronchial epithelial cell line, BEAS-2B, in vitro (Koyama et al., 2002b); however, little is known about the regulation of VEGF and VEGF receptors in the airway epithelium in response to CS exposure of various durations in vivo. In particular, terminal bronchioles are known to play a critical role in a variety of smoking-related lung diseases (Vial, 1986; Hogg et al., 2004), and they are the major sites of airflow limitation in COPD (Hogg et al., 1968; Yanai et al., 1992). We hypothesized that the development of COPD would be associated with changes in the expressions of VEGF and VEGF receptors in the airway epithelium. In the present study, the effects of short- and long-term CS exposure on the expressions of VEGF and VEGF receptors were examined in mouse terminal bronchiolar epithelial cells harvested by laser capture microdissection (LCM). Additionally, the gene expressions of VEGF and VEGF receptors were determined in the subsegmental bronchial epithelial cells collected by bronchoscopic brushing and in bronchiolar epithelial cells harvested by LCM from lifelong nonsmokers, smokers without COPD, and smokers with COPD. VEGF expression was also evaluated at the protein level using immunohistochemistry or an enzyme-linked immunosorbent assay (ELISA).

METHODS

CS-Exposed Mice

We purchased male C57BL/6J mice, 9–10 wk of age, from Charles River Laboratories Japan (Atsugi, Japan). The mice were housed in plastic cages separated from the smoking system, fed on Rodent Diet CE-2 (CLEA Japan, Tokyo), and had free access to water ad libitum. The cages were changed and washed twice per week for sanitation. The experimental groups of mice were moved to wire mesh cages only during CS exposure. Mice were exposed to whole-body mainstream CS generated from commercially available filtered cigarettes (Marlboro, 12 mg tar/1.0 mg nicotine; Philip Morris, Richmond, VA) by the INH06-CIGR0A smoking system (MIPS Co., Osaka, Japan). We used fresh cigarettes purchased within 1 mo before use throughout the experiments. We used the following experimental settings: 35 ml of stroke volume and 15.5 puffs/min to generate CS. The CS was diluted with filtered air at a 1:7 ratio and directed into the exposure chamber (50 (L) × 50 (W) × 25 (H) cm) at a smoke to air ratio of 1:2 (the ratio of final dilution was 1:14). The box was fitted with an exhaust vent of the same size as the blower vent in order to avoid accumulation of mainstream smoke. To confirm adequate CS exposure, the levels of plasma cotinine were measured using a quantitative enzyme immunoassay kit (Salimetrics, State College, PA), as described previously (Dhar et al., 2004). Cotinine was essentially undetectable in mice unexposed to CS (<5 ng/ml). However, following a single 90-min CS exposure, a dramatic increase in plasma cotinine levels was detected ($n = 3$, 173.0 ± 32.4 ng/ml), which was reduced 6 h after CS exposure ($n = 3$, 28.6 ± 4.7 ng/ml). Those levels were similar to that detected in blood samples of mice following CS exposure (Obot et al., 2004) and in blood samples of humans who smoke >5 cigarettes a day (Jarvis et al., 2003). According to some preliminary experiments, we have chosen the protocol of 90-min CS exposure per day because all the mice tested were able to tolerate up to 10 days and resulted in peribronchiolar accumulation of inflammatory cells (unpublished observation). In the short-term CS exposure model, the mice were exposed daily to CS for 90 min/day for 3, 7, or 10 days. In the long-term CS exposure model, the mice were also exposed to CS for 90 min/day, 6 days/wk for up to 24 wk. Age-matched control mice were exposed to filtered air under the same experimental conditions as CS-exposed mice. All animal procedures were performed and the animal's microbiological status was routinely monitored in accordance with the regulations of the Animal Care and Use Committee of the Teijin Institute for Biomedical Research.

Morphometric Assessment

After exposure to CS for various periods (4, 12, 18, and 24 wk), alveolar size of the lung ($n = 6$ per group) was assessed using the previously described morphometric chord length assessment method (Thurlbeck, 1967). In brief, the lungs were inflated by instilling 10% neutralized formaldehyde at a constant pressure of 25 cm H_2O. The lungs were then removed, fixed, and embedded in paraffin. The mid-sagittal sections of the lungs were stained with hematoxylin and eosin (HE), and four rectangular fields (595 μm × 794 μm) were randomly sampled in each mouse. Paralleled lines spaced at 99 μm were overlaid onto each field, and each chord length that defined as the distance between alveolar walls was measured using a computerized color image analysis software system (WinROOF version 5.0, Mitani Co., Fukui, Japan). Chords of airways and vessels were manually

excluded. Mean chord length of each animal was calculated as the average of all of the chord lengths.

Collection of Mouse Bronchiolar Epithelial Cells by LCM

At 24 h after CS exposure, the mice were exsanguinated by severing the abdominal aorta under anesthesia with urethane and α-chloralose. At each time point, six mice were analyzed. The trachea was cannulated with a 22-gauge needle, and the lungs were inflated with diluted Tissue-Tek OCT (Sakura Finetek U.S.A., Torrance, CA) (50% v/v in ribonuclease (RNase)-free phosphate-buffered saline (PBS) containing 10% sucrose), removed from the thoracic cavity, and immediately frozen on dry ice as previously described (Betsuyaku et al., 2001). To retrieve cells within 100 μm of the bronchoalveolar junction, LCM was performed on 7-μm frozen sections using the PixCell II System (Arcturus Engineering, Mountain View, CA) with the following parameters: laser diameter, 30 μm; pulse duration, 5 ms; and amplitude, 50 mW, as described previously (Betsuyaku et al., 2001). After the samples were captured on transfer films (CapSure Macro LCM Caps, LCM0211; Arcturus Engineering), nonspecific attached components were removed with adhesive tape (CapSure Cleanup Pad, LCM0206; Arcturus Engineering). Approximately 10,000 laser bursts were used to collect cells for RNA isolation from each mouse.

Subjects

Two sets of subjects were recruited: one for the bronchoscopic brushing study and the other for the surgical tissue study. For the bronchoscopic brushing study, 6 lifelong nonsmokers, 5 current smokers without COPD, and 15 smokers with COPD (9 current and 6 former smokers) were enrolled (Table 1). For the surgical tissue study, 40 patients who had lung resection for small peripheral tumors were recruited; 14 were lifelong nonsmokers, 14 were smokers without COPD (4 current and 8 former smokers), and 12 were smokers with COPD (all former smokers) (Table 2). Some patients had been subjects in our previous study (Fuke et al., 2004). No age differences were observed among the three groups enrolled in the two studies.

All subjects completed a smoking history questionnaire. Former smokers were arbitrarily defined as people who had quit smoking for at least 1 mo. Measurements of vital capacity and of forced expiratory volume in 1 s were obtained from all subjects. High-resolution computed tomography (HRCT) scans were done in all subjects, and the presence of low-attenuation areas on HRCT was visually ascertained. Most of the COPD subjects (14 subjects in the bronchoscopic brushing study and all of the subjects in the surgical tissue study) had pulmonary emphysema on HRCT. The guideline of the Global Initiative for Obstructive Lung Disease (GOLD) was used to diagnose and grade COPD severity (Fabbri et al., 2004). None of the subjects had a history of asthma, and none of subjects met the criteria for chronic bronchitis, which is defined as the presence of chronic productive cough for 3 mo in each of 2 successive years. None of the patients had an upper-respiratory-tract infection in the preceding month. Written informed consent was obtained from each subject, and the Ethics Committee of Hokkaido University School of Medicine approved the two study protocols.

TABLE 1
Characteristics of the bronchoscopic brushing study subjects

	Lifelong nonsmokers	Smokers without COPD	Smokers with COPD
n	6	5	15
Gender, M/F	6/0	5/0	15/0
Age, yr	68 ± 3	61 ± 2	69 ± 2
Smoking history			
pack-years	0	48 ± 9	61 ± 7
current/former	—	5/0	9/6
FEV_i/FVC, %	79 ± 4	78 ± 2	49 ± 4***
FEV_i, % predicted	122 ± 10	112 ± 11	70 ± 7***
GOLD stage, I/II/III/IV	—	—	6/5/3/1
Differential cell counts at the bronchus			
Total number, $\times 10^6$	4.0 ± 1.3	4.0 ± 0.5	2.8 ± 0.4
epithelial cells, %	97.1 ± 0.8	97.0 ± 0.7	97.7 ± 0.6
neutrophils, %	1.3 ± 0.8	0.8 ± 0.3	0.9 ± 0.3
lymphocytes, %	0.6 ± 0.1	0.8 ± 0.5	0.3 ± 0.1
macrophages, %	1.0 ± 0.4	1.3 ± 0.4	0.7 ± 0.2
eosinophils, %	0.1 ± 0.1	0.1 ± 0.1	0.5 ± 0.4

*: $p < 0.05$ vs. lifelong nonsmokers, **:$p < 0.05$ vs. smokers without COPD (mean ± SE).

Collection of Human Bronchial Epithelial Cells by Bronchoscopic Brushing

All of the current smokers who were enrolled in the bronchoscopic brushing study had stopped smoking cigarettes >12 h

TABLE 2
Characteristics of the surgical tissue study subjects

	Lifelong nonsmokers	Smokers without COPD	Smokers with COPD
n	14	14	12
Gender, M/F	3/11	9/5	12/0
Age, yr	62 ± 3	64 ± 3	66 ± 3
Smoking history			
pack-years	0	47 ± 12	68 ± 7
current/former	—	4/10	0/12
FEV_1/FVC, %	79 ± 2	81 ± 1	59 ± 3***
FEV_1, % predicted	113 ± 5	113 ± 6	90 ± 8
GOLD stage, I/II/III/IV	—	—	10/1/0/1

*:$p < 0.05$ vs. lifelong nonsmokers, **:$p < 0.05$ vs. smokers without COPD (mean ± SE).

prior to the procedure. A BF-1T200 bronchoscope (Olympus, Tokyo) was used for bronchoscopy. The airway mucosal surface was brushed several times at the fourth or fifth branches of the subsegmental bronchi in the right lower lobe using a 2-mm disposable brush (Olympus). The collected cells were suspended in RPMI 1640 medium (GIBCO, Grand Island, NY), and the red blood cells were removed with red blood cell lysing buffer (Sigma, St. Louis, MO). The recovered cells were washed twice in Hanks buffered saline solution (HBSS) without calcium and magnesium (GIBCO). The cytospin preparations were stained using Diff-Quik stain (Kokusai Shiyaku, Kobe, Japan).

Sampling of Human Bronchiolar Epithelial Cells by LCM

Six or more blocks of peripheral lung tissue (1.0 cm × 1.0 cm × 0.5 cm) were collected in areas that were remote from the tumor and frozen using dry ice as soon as possible after lung resection (Fuke et al., 2004). LCM of the bronchiolar epithelial cells was performed on hematoxylin-stained peripheral lung tissue using a PixCell II System as described above. The bronchiolar epithelial cells were retrieved from the terminal bronchiole and proximally along airways up to approximately 500 μm in diameter. At least 6 bronchioles were randomly selected, and a total of 40,000 laser bursts was used to collect cells from each subject.

RNA Purification and 5′-Exonuclease-Based Fluorogenic PCR

Total RNA was extracted using an RNeasy Mini kit (Qiagen, Hilden, Germany). The quantity and quality of the RNA were determined using a LabChip kit (Agilent Technologies, Palo Alto, CA). Reverse transcription and 5′-exonuclease–based fluorogenic polymerase chain reaction (PCR) was carried out using the ABI PRISM 7700 (Applied Biosystems, Foster City, CA), as described previously (Fuke et al., 2004; Betsuyaku et al., 2001; Betsuyaku et al., 2004). Taqman Gene Expression Assays probes (Applied Biosystems) were used for VEGF (Assay ID; Hs00173626_m1), VEGFR-1 (Hs00176573_m1), and VEGFR-2 (Hs00176676_m1); the levels were normalized against mouse β2-microglobulin mRNA or human glyceraldehyde-3-phosphatase dehydrogenase (GAPDH) mRNA.

Assessment of VEGF mRNA Isoforms

The reverse-transcription PCR (RT-PCR) of the mRNA encoding the 121-, 165- and 189-amino acid isoforms of VEGF results in PCR products with 403, 535, and 607 base pairs (bp), respectively, based on the primers spanning the insertion/deletion site of VEGF165 that were previously designed (Nagai et al., 2005). PCR was carried out as previously described; β-actin was used as an endogenous control (Nagai et al., 2005). The PCR products were separated using 2% agarose gel electrophoresis.

Measurement of VEGF Protein in the Bronchial Epithelial Cells

VEGF protein could be quantified for 24 of the 26 subjects at the subsegmental bronchial epithelium level, since only a limited number of cells could be obtained by brushing in some subjects. Brushed epithelial cells were lysed by freezing and thawing in 0.9% saline (2×10^6 cells/ml), and the VEGF levels were quantified using an ELISA kit (Amersham, Little Chalfont, UK). The ELISA was designed for measuring VEGF165 and VEGF121 levels. Total protein was quantified using the BCA assay (Pierce, Rockford, IL); in each sample, the VEGF levels were normalized against the total protein concentration.

Immunohistochemistry

Frozen lung tissues were sectioned at 5 μm in a cryostat (Leica, Nussloch, Germany), placed on poly-L-lysine-coated glass slides (Matsunami, Osaka, Japan), air-dried, and then fixed in 4% paraformaldehyde for 10 min. After blocking with 3% goat serum and 3% skim milk, the sections were incubated at 4°C overnight with 1:100 anti-VEGF rabbit polyclonal antibody (sc-507; Santa Cruz Biotechnology, Inc., Santa Cruz, CA), as previously reported (Fehrenbach et al., 1999; Kranenburg et al., 2005). Normal rabbit immunoglobulin fraction (DakoCytomation, Glostrup, Denmark) was used as a negative control and resulted in no tissue staining. Color detection was performed using an antifade medium (VECTASTAIN ABC kit; Vector Laboratories, Burlingame, CA) with an alkaline phosphatase substrate (Vector Laboratories). Sections were counterstained with nuclear fast red (Vector Laboratories), dehydrated in graded ethanol, cleaned with xylene, and then mounted.

Semiquantitative Scoring of Immunohistochemistry

One peripheral lung tissue section, in which at least one bronchiolar structure could be identified (median 2.5 bronchioles, range 1–8), was assessed per subject. In order to avoid run-to-run variations in the immunoreaction, all specimens were stained during the same run. For the quantitative analyses, the entire section of a tissue block was assessed and scored at the same magnification for each subject. The VEGF expression level in each bronchiole was analyzed semiquantitatively using a visual scoring method with grades ranging from 0 to 3 (0 = no staining; 1 = moderate staining; 2 = intense staining; 3 = very intense staining), as previously described by de Boer et al. (2000); an average score was then calculated. Scoring was performed in a blinded manner; the observers were unaware of the subjects' clinical details. The staining intensity was scored by two independent observers (M.S. and S.F), and the average scores were analyzed. The correlation coefficient of the staining scores between observers was .82 (Pearson's correlation analysis, $p < .001$).

Data Presentation and Statistical Analysis

Demographic, morphometric, and immunohistochemical data are expressed as means ± standard error (SE). Differences

between two groups were analyzed using a two-tailed unpaired t-test; more than two groups were compared using single-factor analysis of variance followed by a post hoc Tukey–Kramer test. The RT-PCR and ELISA data are expressed as the median and range. Differences between the two groups were analyzed using the Mann–Whitney U-test, and more than two groups were compared using the Kruskal–Wallis test followed by the Mann–Whitney U-test. Correlations were analyzed using Spearman's rank correlation test. All tests were performed using the StatView J 5.0 System (SAS Institute, Inc., Cary, NC). Statistical significance was set at $p < .05$.

RESULTS

VEGF and VEGF Receptor Levels in Bronchiolar Epithelial Cells in the Short-Term CS Exposure Mouse Model

To determine whether short-term CS exposure affects gene expression levels of VEGF and VEGF receptors in the airway epithelial cells, mice were exposed to CS daily for up to 10 days. The expressions of VEGF, VEGFR-1, and VEGFR-2 were quantified in LCM-retrieved terminal bronchiolar epithelial cells. The bronchiolar VEGF expression tended to be downregulated, but this was not statistically significant during the 10 days of CS exposure (Figure 1a). In contrast, compared to unexposed mice, a significant decrease was observed at 3, 7, and 10 days for VEGFR-1 and at 10 days for VEGFR-2 ($p < .05$, respectively) (Figure 1, b and c).

VEGF and VEGF Receptors in Bronchiolar Epithelial Cells in the Long-Term CS Exposure Mouse Model

To determine whether long-term CS exposure affects gene expression levels of VEGF and VEGF receptors in the airway epithelial cells, mice were exposed to CS for up to 24 wk. Destruction of alveolar walls, enlargement of alveolar ducts, and accumulation of inflammatory cells were observed at 24 wk of CS exposure, but not in the age-matched controls (Figure 2,a and b). At 4 wk of CS exposure, a significant increase in the mean chord length was noted ($p < .001$) (Figure 2c), and bronchiolar VEGF, VEGFR-1, and VEGFR-2 expressions were significantly downregulated compared to controls. The significant reductions in VEGF, VEGFR-1, and VEGFR-2 were maintained for up to 24 wk of CS exposure ($p < .05$) (Figure 3). On immunohistochemistry, it was confirmed that bronchiolar VEGF was also decreased at the protein level in mice exposed to long-term CS (Figure 4).

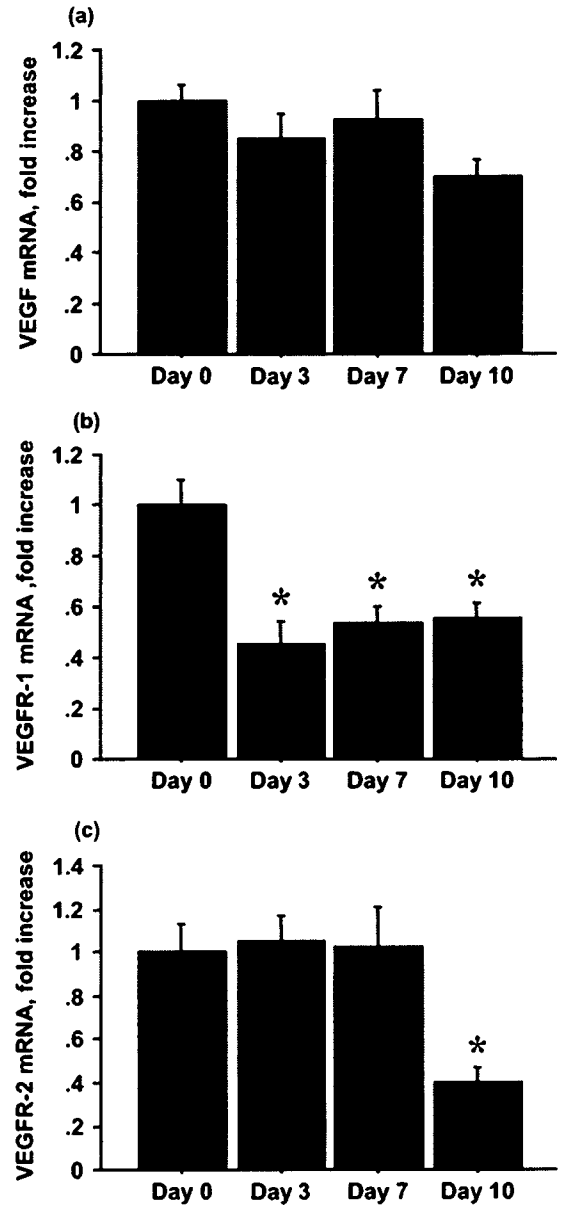

FIG. 1. VEGF, VEGFR-1, and VEGFR-2 expressions in bronchiolar epithelium in mice with short-term CS exposure. (a) VEGF mRNA. (b) VEGFR-1 mRNA. (c) VEGFR-2 mRNA. The data are plotted as means ± SE ($n = 6$ per group). The values are corrected for β2-microglobulin and expressed as fold increases against the mean value of day 0. Asterisk indicates statistical significance at $p < .05$ compared to day 0.

VEGF and VEGF Receptors in Human Bronchial Epithelial Cells

The expressions of VEGF and VEGF receptors in human airway epithelial cells and their relationship with smoking and the presence of COPD were investigated. The assessment of the subsegmental bronchial epithelial cells collected by bronchoscopic brushing showed that smokers with COPD had a significantly decreased VEGF mRNA expression compared to lifelong nonsmokers ($p = .01$) and to smokers without COPD ($p = .02$) (Figure 5a). In these cells, VEGF protein levels were also significantly decreased in smokers with COPD compared to lifelong nonsmokers ($p = .02$); however, the difference between smokers with and without COPD was not statistically

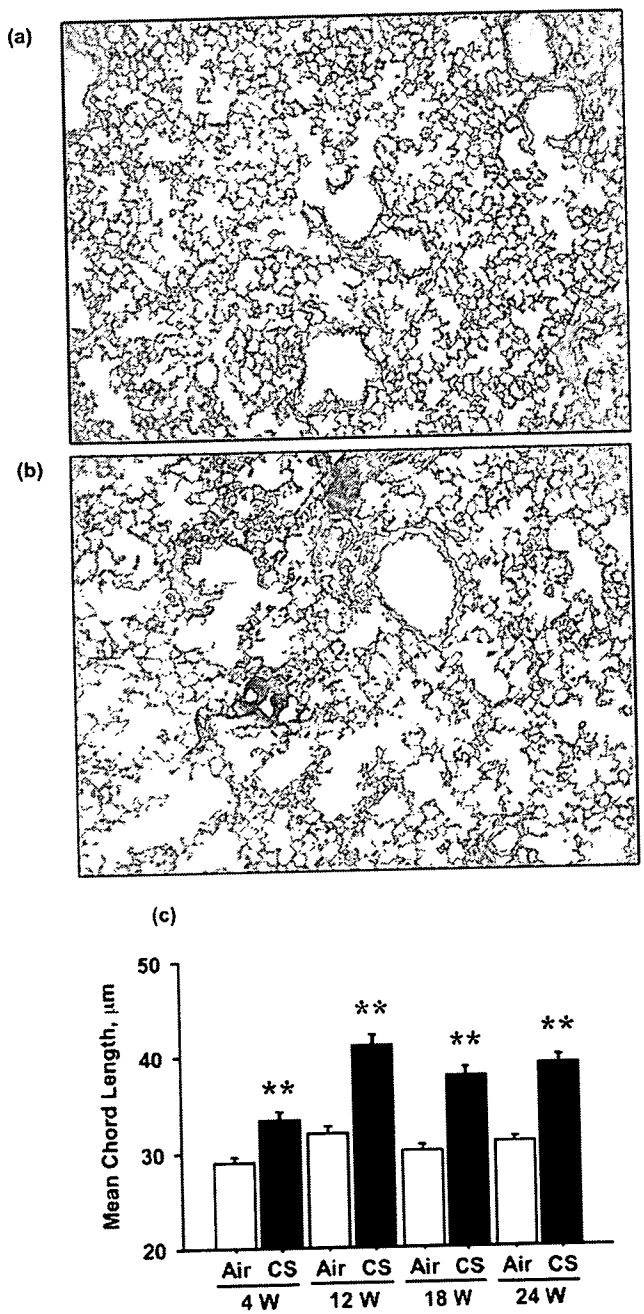

FIG. 2. Development of emphysematous changes in mice with long-term CS exposure. Representative HE-stained lung sections of control mice (a) and CS-exposed mice at 24 wk (b). Original magnification, 100×. (c) Mean chord length. The data are plotted as means ± SE ($n = 6$ per group). Double asterisk indicates statistical significance at $p < .001$ compared to control mice at each time point.

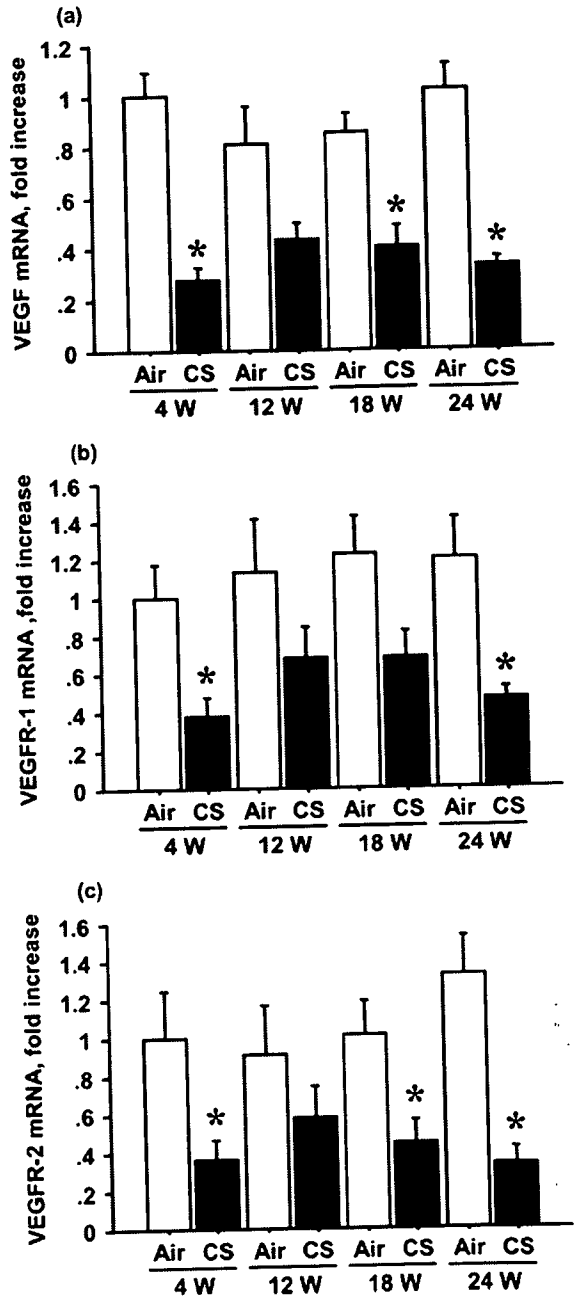

FIG. 3. VEGF, VEGFR-1, and VEGFR-2 expressions in bronchiolar epithelium in mice with long-term CS exposure. (a) VEGF mRNA. (b) VEGFR-1 mRNA. (c) VEGFR-2 mRNA. The data are plotted as means ± SE ($n = 6$ per group). Values are corrected for β2-microglobulin and expressed as fold increases against the mean value of control mice at 4 wk. Asterisk indicates statistical significance at $p < .05$ compared to control mice at each time point.

significant ($p = .08$) (Figure 5b). It was found that VEGF121 and VEGF165 were the major isoforms of VEGF mRNA expressed in the bronchial epithelial cells, and that both of these isoforms were substantially reduced in smokers with COPD (Figure 5c). VEGFR-2 mRNA levels did not differ among the three groups (data not shown). VEGFR-1 mRNA expressions were below the detection level in most of the subsegmental bronchial samples (data not shown).

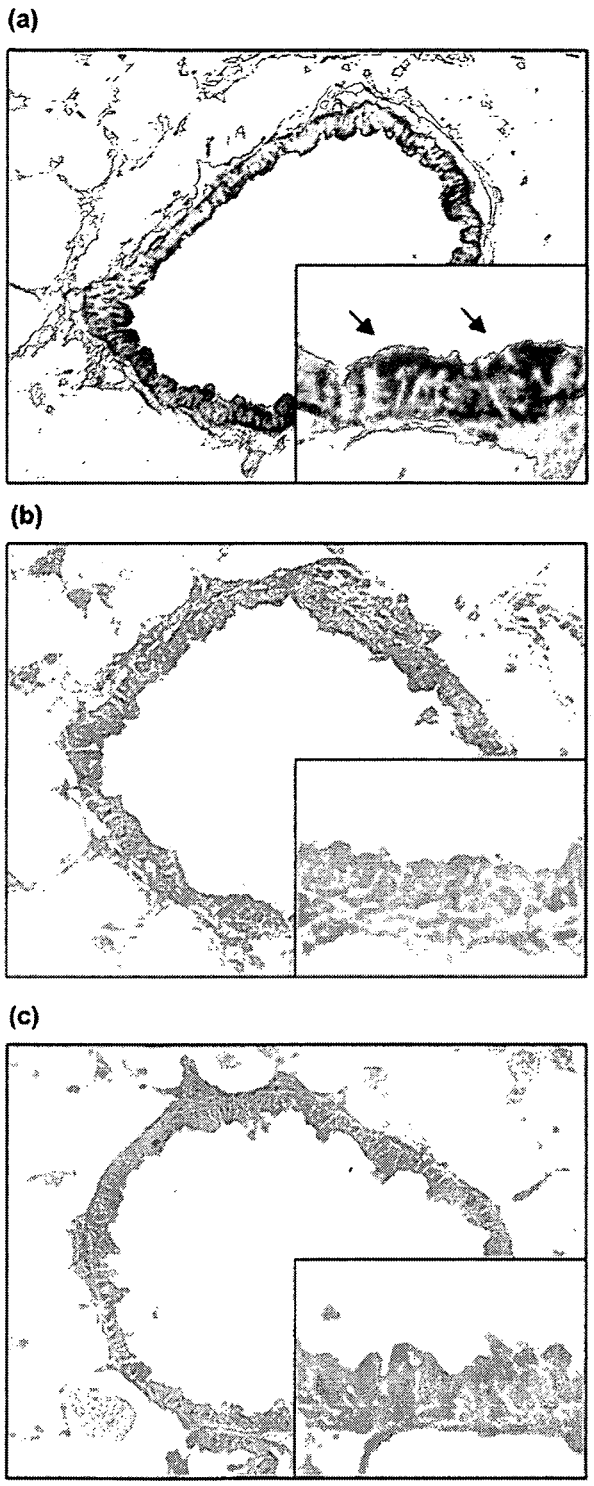

FIG. 4. Immunohistochemistry for VEGF in terminal bronchioles of mice. (a) Unexposed control mouse, (b) a mouse exposed to CS for 4 wk, and (c) a mouse exposed to CS for 24 wk. Positive immunohistochemical staining appears blue-purple (arrows). Original magnification, 200×. The magnified views of the bronchiolar epithelium are shown in the inset of each figure.

VEGF and VEGF Receptors in Human Bronchiolar Epithelial Cells

In the surgical tissue study, it was found that VEGF mRNA levels in the bronchiolar epithelium harvested by LCM were significantly decreased in smokers with COPD compared to lifelong nonsmokers ($p < .001$) and to smokers without COPD ($p = .006$) (Figure 6a). VEGF protein levels evaluated by immunohistochemistry were significantly decreased in smokers with COPD compared to lifelong nonsmokers ($p = .01$) and to smokers without COPD ($p < .001$) (Figure 6, b and c). Compared to lifelong nonsmokers, VEGFR-2 mRNA expression levels were also reduced in smokers with and without COPD ($p < .001$ and $p = .03$, respectively), although the difference between smokers with and without COPD was not statistically significant ($p = .05$) (Figure 6d). VEGFR-1 mRNA expression levels in the bronchiolar epithelial cells did not differ among the three groups (data not shown).

DISCUSSION

First, it was demonstrated that CS induced downregulation of VEGF and both of its receptors in the bronchiolar epithelium prior to the development of emphysema in mice. Furthermore, it was found that bronchial and bronchiolar VEGF was decreased in COPD patients, while VEGFR-2 was downregulated in the bronchiolar epithelium in smokers regardless of whether or not they had COPD.

Although VEGF is well known as a survival factor for endothelial cells (Ferrara et al., 2003), the function of VEGF and VEGF receptors in epithelial cells is largely unknown. Recently, some studies have suggested that VEGF is also a survival factor for epithelial cells in an autocrine manner (Brown et al., 2001; Foster et al., 2003; Mura et al., 2007). Of particular note in the present study is that even short-term CS exposure in mice led to downregulation of both VEGF receptors, but not VEGF; this suggests that the receptors are more prone to being downregulated in response to CS than VEGF. In the long-term CS exposure mouse model, the enlargement of alveolar size was noted at as early as 4 wk of CS exposure; this appears to be notably earlier than in previous studies using the same strain of mice, C57BL/6J (Takubo et al., 2002; Bartalesi et al., 2005). Importantly, along with the development of emphysema, VEGF, as well as VEGFR-1 and VEGFR-2, was already significantly downregulated in bronchiolar epithelium at 4 wk.

A previous report showed a decrease of whole lung VEGF and VEGFR-2 expressions following chronic CS exposure in rats (Marwick et al., 2006). However, little attention has been given to determining the lung cell types in which VEGF expression might be changed or the role that VEGFR-1 plays in CS-induced emphysema. It has been reported that the administration of SU5416, an inhibitor of both VEGFR-1 and VEGFR-2, led to emphysema in adult rat lungs (Kasahara et al., 2000), while specific inhibition of VEGFR-2 with NVP-AAD777 did not result

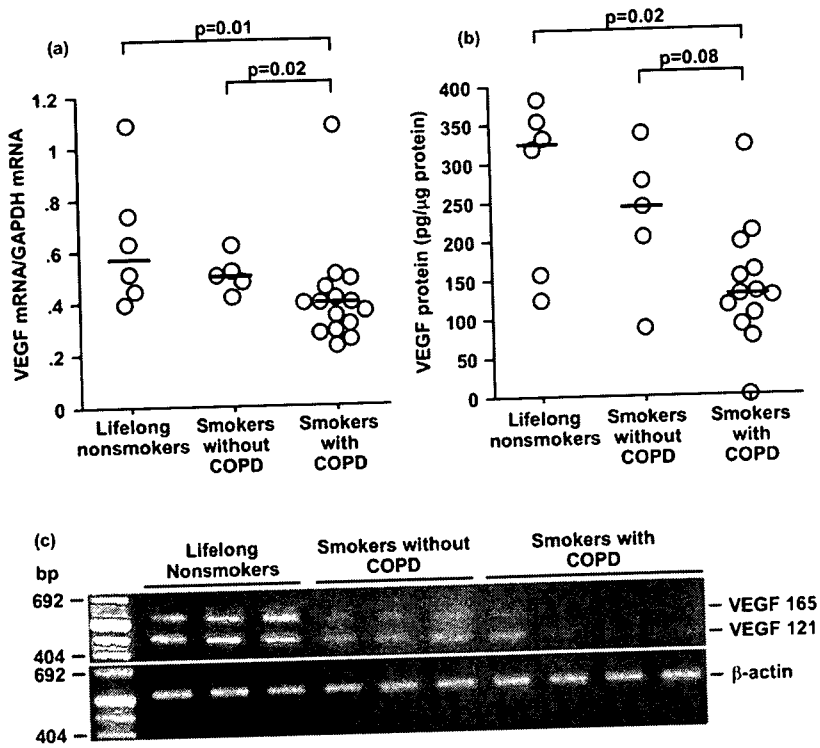

FIG. 5. VEGF expression in human bronchial epithelial cells. (a) VEGF mRNA corrected for GAPDH mRNA. (b) VEGF protein (pg/μg protein). Medians are indicated by horizontal lines. (c) Bronchial epithelial cells produced PCR products of 403 and 535 bp, corresponding to the 121- and 165-amino acid isoforms of VEGF, respectively. VEGF189 expression was barely detected. PCR products for β-actin (513 bp) served as an endogenous control for each sample. Representative samples from lifelong nonsmokers, smokers without COPD, and smokers with COPD are shown.

in the development of emphysema (Marwick et al., 2006). In the adult mouse lung, the pulmonary stem cell population has been identified and isolated at the bronchioalveolar duct junction. Thus, bronchiolar epithelium is thought to be important for lung tissue repair and homeostasis (Kim et al., 2005). Taken together with the current findings, the CS-induced downregulation of both VEGF receptors and VEGF might cause impaired VEGF signaling in bronchiolar epithelium, which would lead to a failure in maintaining these cell populations. This would consequently have detrimental effects on the integrity of alveolar structure in mice. However, the experimental results should be interpreted with caution, since our method of CS exposure is different in condition, including puffing profile and duration of exposure per day, from the previous studies (Obot et al., 2004), and is apparently different from that of human smokers.

Of note, bronchioles play a critical role in a variety of smoking-related lung diseases in humans (Hogg et al., 2004), and they are the major sites of airflow limitation in COPD (Hogg et al., 1968; Yanai et al., 1992). In the present study, it was found that VEGF expression was decreased in both bronchial and bronchiolar epithelial cells in COPD patients, while bronchiolar VEGFR-2 was downregulated in smokers regardless of whether or not they had COPD. We recently reported that the same population of cells that line the bronchioles of mild COPD patients exhibit upregulation of inflammatory chemokines, such as interleukin-8, and downregulation of catalase, an antioxidant, as well as several heat-shock protein 70 family chaperones (Fuke et al., 2004; Betsuyaku et al., 2006). The presence of cellular oxidative stress due to an oxidant–antioxidant imbalance and impaired VEGF-VEGFR-2 axis signaling may in turn result in several adverse cellular events only in susceptible smokers with long-term smoking histories (Rahman, 2005). In contrast to mouse bronchiolar cells, human bronchial and bronchiolar epithelial cells express only very low VEGFR-1 mRNA levels. This discrepancy would be the result of interspecies differences, in that Clara cells are approximately 90% of the cells that line mouse terminal airways (Plopper, 1997).

In sharp contrast to the present study, Kranenburg et al., using immunohistochemistry, reported significantly increased VEGF levels in the bronchiolar epithelial cells of COPD (Kranenburg et al., 2005). Although the discrepancy between the two studies cannot be fully explained, it may be due to differences in the subjects' characteristics. For example, all smokers with COPD in the present surgical tissue study had emphysema on HRCT and did not have chronic bronchitis, while the COPD group in the study by Kranenburg et al. included subjects with chronic bronchitis. This discrepancy would be in line with the previous findings that sputum

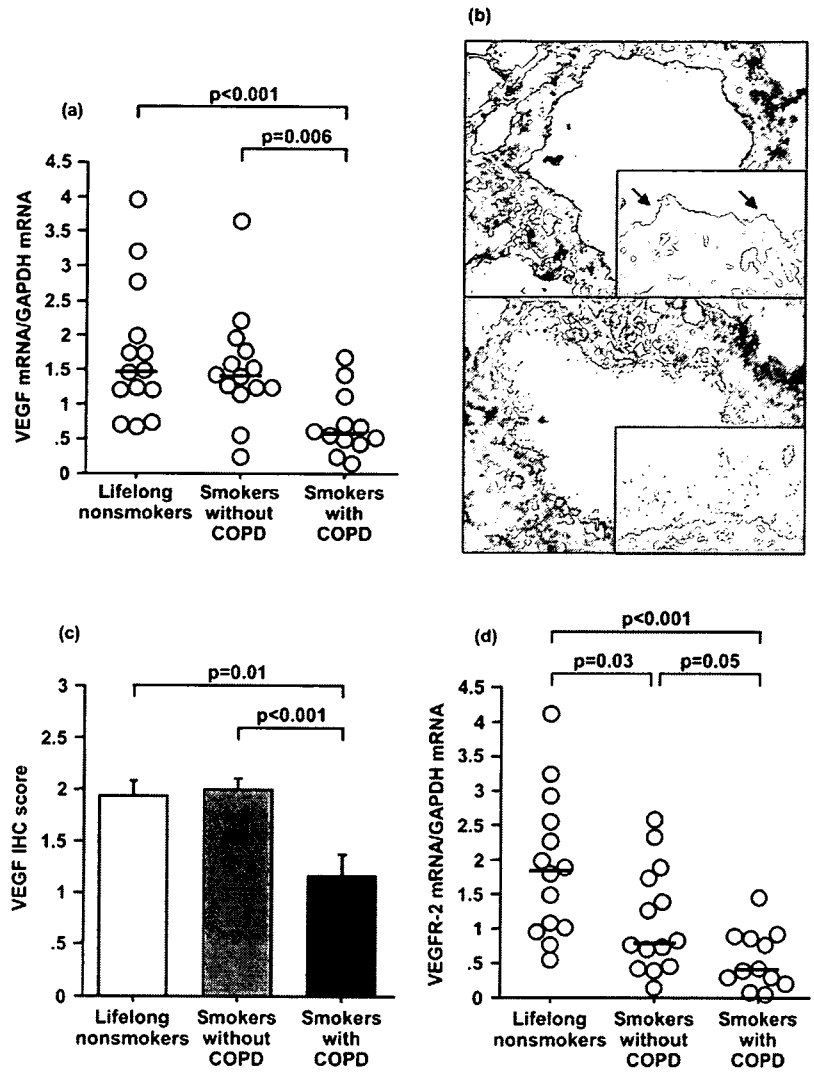

FIG. 6. VEGF and VEGFR-2 expressions in human bronchiolar epithelial cells. (a) VEGF mRNA corrected for GAPDH mRNA. Medians are indicated by horizontal lines. (b) Immunohistochemistry for VEGF protein. Terminal bronchioles from a lifelong nonsmoker (upper) and a smoker with COPD (lower), in which the bronchiolar epithelium is magnified in the insets, are shown. Positive immunohistochemical staining appears blue–purple (arrows). Original magnification, 200×. (c) VEGF protein expression in bronchiolar epithelium was semiquantified using a visual scoring method with grades ranging from 0 to 3. The data are plotted as means ± SE. (d) VEGFR-2 mRNA corrected for GAPDH mRNA. Medians are indicated by horizontal lines.

VEGF levels were higher in patients with chronic bronchitis (Kanazawa et al., 2003; Rovina et al., 2007), but lower in patients with emphysema (Kanazawa et al., 2003). The decrease of VEGF at both mRNA and protein levels was confirmed in the present study using quantitative RT-PCR coupled with ELISA or immunohistochemistry.

In the present study, epithelial cells were collected with more than 97% purity by bronchoscopic brushing, and LCM, which harvests the bronchiolar epithelium very well, was used (Fuke et al., 2004; Betsuyaku et al., 2001, 2004). However, it should be noted that the cells that were harvested were likely a mixture of various epithelial cell types that were present at a given level. Epithelial heterogeneity in the airways could be important under certain circumstances, such as COPD. The results in this study emphasize the importance of doing gene expression analysis for each lung tissue compartment in vivo in order to overcome the weakness of gene expression analysis using whole lung tissue. However, to investigate gene expression in specific epithelial cell types, more precise cell isolation using specific targeting is required.

The present study has some limitations. First, there was considerable variation in the smoking status among the smokers.

The decrease of VEGFR-2 expression levels in the bronchiolar epithelium implies that VEGF signaling via VEGFR-2 might be suppressed to some degree solely by chronic cigarette smoke exposure, even in the absence of disease. Although there was no significant difference in pack-years of smoking between the two groups of smokers, the amount of cigarette smoking may influence gene expression per se. Second, most of the smokers with COPD that were recruited into the surgical tissue study had only mild COPD (GOLD stage I). To obtain a better understanding of the involvement of VEGF signaling in the mechanism of disease progression, a larger sample of patients with more advanced disease should be assessed. Nevertheless, the findings suggest that changes in VEGF signaling may be important in the development of even mild forms of COPD and/or emphysema. Third, all of the smokers with COPD were male, and we used only male mice in the animal study. Considering that men and women may be phenotypically different in their response to tobacco smoke and gender difference could influence the pathophysiology of COPD (Han et al., 2007), our findings might not to be extrapolated to females, and the gender issue remains to be elucidated.

In summary, it was found that CS exposure downregulated the expressions of VEGF and VEGF receptors in mouse bronchiolar epithelium prior to and during the development of emphysema. Furthermore, it was also noted that VEGF levels were decreased in airway epithelial cells of COPD patients. A further analysis of cell-specific regulation of VEGF signaling will provide new insights into COPD and/or emphysema.

REFERENCES

Bartalesi, B., Cavarra, E., Fineschi, S., Lucattelli, M., Lunghi, B., Martorana, P. A., and Lungarella, G. 2005. Diffrernt lung responses to cigarette smoke in two strains of mice sensitive to oxidants. *Eur. Respir. J.* 25:15–22.

Berse, B., Brown, L. F., Van de Water, L., Dvorak, H. F., and Senger, D. R. 1992. Vascular permeability factor (vascular endothelial growth factor) gene is expressed differently in normal tissues, macrophages, and tumors. *Mol. Biol. Cell* 2:211–220.

Betsuyaku, T., and Senior, R. M. 2004. Laser capture microdissection and mRNA characterization of mouse airway epithelium: Methodological considerations. *Micron* 35:229–234.

Betsuyaku, T., Griffin, G. L., Watson, M. A., and Senior, R. M. 2001. Laser capture microdissection and real-time reverse transcriptase/polymerase chain reaction of bronchiolar epithelium after bleomycin. *Am. J. Respir. Cell Mol. Biol.* 25:278–284.

Betsuyaku, T., Fuke, S., Nasuhara, Y., Morikawa, T., Kondo, S., and Nishimura, M. 2006. Diverse Expression of antioxidants and inflammatory chemokines in terminal bronchiolar epithelium in chronic obstructive pulmonary disease. *Proc. Am. Thorac. Soc.* 3:471–472.

Brown, K. R., England, K. M., Goss, K. L., Snyder, J. M., and Acarregui, M. J. 2001. VEGF induces airway epithelial cell proliferation in human fetal lung in vitro. *Am. J. Physiol. Lung Cell Mol.* 281:L1001–L1010.

de Boer, W. I., Sont, J. K., van Schadewijk, A., Stolk, J., van Krieken, J. H., and Hiemstra, P. S. 2000. Monocyte chemoattractant protein 1, interleukin 8, and chronic airways inflammation in COPD. *J. Pathol.* 190:619–626.

Dhar, P. 2004. Measuring tobacco smoke exposure: quantifying nicotine/cotinine concentration in biological samples by colorimetry, chromatography and immunoassay methods. *J. Pharm. Biomed. Anal.* 35:155–168.

Fabbri, L., Pauwels, R. A., and Hurd, S. S. 2004. Global strategy for the diagnosis, management and prevention of chronic obstructive pulmonary disease: GOLD executive summary updated 2003. *J. COPD* 1:105–141.

Fehrenbach, H., Kasper, M., Haase, M., Schuh, D., and Muller, M. 1999. Differential immunolocalization of VEGF in rat and human adult lung, and in experimental rat lung fibrosis: light, fluorescence, and electron microscopy. *Anat. Rec.* 254:61–73.

Ferrara, N., Gerber, H. P., and LeCouter, J. 2003. The biology of VEGF and its receptors. *Nat. Med.* 9:669–676.

Foster, R. R., Hole, R., Anderson, K., Satchell, S. C., Coward, R. J., Mathieson, P. W., Gillatt, D. A., Saleem, M. A., Bates, D. O., and Harper, S. J. 2003. Functional evidence that vascular endothelial growth factor may act as an autocrine factor on human podocytes. *Am. J. Physiol. Renal. Physiol.* 284:F1263–F1273.

Fuke, S., Betsuyaku, T., Nasuhara, Y., Morikawa, T., Katoh, H., and Nishimura, M. 2004. Chemokines in bronchiolar epithelium in the development of chronic obstructive pulmonary disease. *Am. J. Respir. Cell Mol. Biol.* 31:405–412.

Han, M. K., Postma, D., Mannino, D., Giardino, N. D., Buist, S., Curtis, J. L., and Martinez, F. J. 2007. Gender and COPD: Why it matters. *Am. J. Respir. Crit. Care Med.* 176:1179–1184.

Hogg, J. C., Macklem, P. T., and Thurlbeck, W. M. 1968. Site and nature of airway obstruction in chronic obstructive lung disease. *N. Engl. J. Med.* 278:1355–1360.

Hogg, J. C., Chu, F., Utokaparch, S., Woods, R., Elliott, W. M., Buzatu, L., Cherniack, R. M., Rogers, R. M., Sciurba, F. C., Coxson, H. O., and Pare, P. D. 2004. The nature of small-airway obstruction in chronic obstructive pulmonary disease. *N. Engl. J. Med.* 350:2645–2653.

Jarvis, M. J., Primatesta, P., Erens, B., Feyerabend, C., and Bryant, A. 2003. Measuring nicotine intake in population surveys: comparability of saliva cotinine and plasma cotinine estimates. *Nicotine Tobacco Res.* 5:349–355.

Kanazawa, H., Asai, K., Hirata, K., and Yoshikawa, J. 2003. Possible effects of vascular endothelial growth factor in the pathogenesis of chronic obstructive pulmonary disease. *Am. J. Med.* 114:354–358.

Kasahara, Y., Tuder, R.M., Taraseviciene-Stewart, L., Le Cras, T. D., Abman, S., Hirsh, P. K., Waltenberger, J., and Voelkel, N. F. 2000. Inhibition of VEGF receptors causes lung cell apoptosis and emphysema. *J. Clin. Invest.* 106:1311–1319.

Kasahara, Y., Tuder, R. M., Cool, C. D., Lynch, D. A., Flores, S. C., and Voelkel, N. F. 2001. Endothelial cell death and decreased expression of vascular endothelial growth factor and vascular endothelial growth factor receptor 2 in emphysema. *Am. J. Respir. Crit. Care Med.* 163:737–744.

Kim, C. F., Jackson, E. L., Woolfenden, A. E., Lawrence, S., Babar, I., Vogel, S., Crowley, D., Bronson, R. T., and Jacks, T. 2005. Identification of bronchioalveolar stem cells in normal lung and lung cancer. *Cell* 121:823–835.

Koyama, S., Sato, E., Haniuda, M., Numanami, H., Nagai, S., and Izumi, T. 2002a. Decerased level of vascular endothelial growth factor in

bronchoalveolar lavage fluid of normal smokers and patients with pulmonary fibrosis. *Am. J. Respir. Crit. Care Med.* 166:382–385.

Koyama, S., Sato, E., Haniuda, M., Numanami, H., Kurai, M., Nagai, S., and Izumi. T. 2002b. Vascular endothelial growth factor mRNA and protein expression in airway epithelial cell lines in vitro. *Eur. Respir. J.* 20:1449–1456.

Kranenburg, A. R., de Boer, W. I., Alagappan, V. K. T., Sterk, P. J., and Sharma, H. S. 2005. Enhanced bronchial expression of vascular endothelial growth factor and receptors (Flk-1 and Flt-1) in patients with chronic obstructive pulmonary disease. *Thorax* 60:106–113.

Marwick. J. A., Stevenson, C. S., Giddings, J., MacNee. W., Butler, K., Rahman, I., and Kirkham, P. A. 2006. Cigarette smoke disrupts the VEGF165-VEGFR2 receptor signaling complex in rat lungs and patients with COPD: Morphological impact of VEGFR2 inhibition. *Am. J. Phisiol. Lung Cell Mol. Physiol.* 290:897–908.

Mura, M., Han, B., Andrade, C. F., Seth, R., Hwang, D., Waddell, T. K., Keshavjee, S., and Liu, M. 2006. The early responses of VEGF and its receptors during acute lung injury: Implication of VEGF in alveolar epithelial cell survival. *Crit. Care* 10:R130.

Nagai, K., Betsuyaku, T., Ito, Y., Nasuhara, Y., and Nishimura M. 2005. Decrease of vascular endothelial growth factor in macrophages from long-term smokers. *Eur. Respir. J.* 25:626–633.

Obot. C., Lee. K., Fuciarelli, A., Renne, R., McKinney, W. 2004. Characterization of mainstream cigarette smoke-induced biomarker responsed in ICR and C57Bl/6 mice. *Inhal. Toxicol.* 16:701–719.

Pauwels, R. A., Buist, A. S., Calverley, P. M., Jenkins. C. R., Hurd, S. S., and GOLD Science Committee. 2001. Global strategy for the diagnosis, management. and prevention of chronic obstructive pulmonary disease. NHLBI/WHO Global Initiative for Chronic Obstructive Lung Disease (GOLD) Workshop summary. *Am. J. Respir. Crit. Care Med.* 163:1256–1276.

Pauwels. R. A., and Rabe, K. F. 2004. Burden and clinical features of chronic obstructive pulmonary disease (COPD). *Lancet* 364:613–620.

Plopper, C. G. 1997. Clara cells. In *Lung growth and development. Lung biology in health and disease*, ed. J. A. McDonald, pp. 181–209. New York: Marcel Dekker.

Rahman, I. 2005. Oxidative stress in pathogenesis of chronic obstructive pulmonoary disease: Cellular and molecular mechanisms. *Cell Biochem. Biophys.* 43:167–188.

Rovina, N., Papapetropoulos, A., Kollintza, A., Michailidou, M., Simoes, D. C., Roussos, C., and Gratziou, C. 2007. Vascular endothelial growth factor: An angiogenic factor reflecting airway inflammation in healthy smokers and in patients with bronchitis type of chronic obstructive pulmonary disease? *Respir. Res.* 8: 53.

Takubo, Y., Guerassimov, A., Ghezzo, H., Triantafillopoulos, A., Bates, J. H., Hoidal, J. R., and Cosio, M. G. 2002. Alpha1-antitrypsin determines the pattern of emphysema and function in tobacco smoke-exposed mice: Parallels with human disease. *Am. J. Respir. Crit. Care Med.* 166:1596–1603.

Tang, K., Rossiter, H. B., Wagner, P. D., and Breen, E. C. 2004. Lung-targeted VEGF inactivation leads to an emphysema phenotype in mice. *J. Appl. Physiol.* 97:1559–1566.

Thurlbeck, W. M. 1967. Internal surface area and other measurements in emphysema. *Thorax* 22:483–496.

Vial, W. C. 1986. Cigarette smoking and lung disease. *Am. J. Med. Sci.* 291:130–142.

Voelkel, N. F., Vandivier, W. V., and Tuder, R. M. 2006. Vascular endothelial growth factor in the lung. *Am. J. Phisiol. Lung Cell Mol. Physiol.* 290:209–221.

Waltenberger, J., Claesson-Welsh, L., Siegbahn, A., Shibuya, M., and Heldin, C. H. 1994. Different signal transduction properties of KDR and Flt1, two receptors for vascular endothelial growth factor. *J. Biol. Chem.* 269:26988–26995.

Yanai, M., Sekizawa, K., Ohrui, T., Sasaki, H., and Takishima, T. 1992. Site of airway obstruction in pulmonary disease: Direct measurement of intrabronchial pressure. *J. Appl. Physiol.* 72:1016–1023.

Available online at www.sciencedirect.com
ScienceDirect
Biochemical and Biophysical Research Communications 368 (2008) 426–432
BBRC
www.elsevier.com/locate/ybbrc

Role of basement membrane in EMMPRIN/CD147 induction in rat tracheal epithelial cells ☆

Takeshi Hosokawa [a,b], Tomoko Betsuyaku [a,*], Nao Odajima [a], Masaru Suzuki [a], Katsumi Mochitate [b], Yasuyuki Nasuhara [a], Masaharu Nishimura [a]

[a] First Department of Medicine, Hokkaido University School of Medicine, N-15, W-7, Kita-ku, Sapporo 060-8638, Japan
[b] Environmental Health Sciences Division, National Institute for Environmental Studies, Tsukuba, Japan

Received 16 January 2008
Available online 1 February 2008

Abstract

Extracellular matrix metalloproteinase inducer (EMMPRIN) is a glycosylated transmembrane protein known to induce matrix metalloproteinases (MMPs). Although the expression of EMMPRIN is physiologically limited to fetal lung epithelium, the transcriptional regulation of this protein remains to be elucidated. We hypothesized that the interaction of epithelial cells with the basement membrane regulates EMMPRIN expression. The basement membrane has highly integrated architecture composed of specific extracellular matrix, such as laminins and type IV collagen, and exhibits multiple functions. We previously developed a structured basement membrane mimic, a synthesized basement membrane (sBM) substratum, in which laminin-111, a unique component of embryonic lungs, is incorporated. In the present study we quantified expression of EMMPRIN mRNA of rat tracheal epithelial cells cultured on sBM, laminin-111, type IV collagen, or laminin-332. EMMPRIN was upregulated on sBM and laminin-111, although this was not accompanied by MMP-9 induction. In contrast, type IV collagen and laminin-332 did not induce EMMPRIN. These findings suggest potential roles for basement membrane in the transcriptional regulation of tracheal epithelial EMMPRIN.

Keywords: EMMPRIN; Extracellular matrix; Laminin; Basement membrane; Type IV collagen; MMP

Extracellular matrix metalloproteinase inducer (EMMPRIN), also known as CD147, basigin, or OX47, is a glycosylated transmembrane protein that has been identified as a member of the immunoglobulin superfamily [1,2]. EMMPRIN is strongly expressed in fetal lung epithelium, suggesting a physiologic role in development, although it is essentially absent in normal adult lungs [3,4]. Pathological upregulation has been reported in lung cancers [5,6], as well as in various malignant tumors [7]. One defining property of EMMPRIN is its capacity to stimulate production of various matrix metalloproteinases (MMPs) by adjacent mesenchymal cells or cancer cells in an autocrine manner [8,9]. We recently reported increased EMMPRIN expression in hyperproliferative bronchiolar epithelial cells or in aberrant re-epithelialization in injured lungs [10–12]. However, the regulatory mechanisms of EMMPRIN expression under physiological and pathological conditions in the lungs are not fully understood.

Basement membrane has a highly integrated architecture composed of specific extracellular matrix (ECM) such as laminin, type IV collagen, entactin/nidogen, and perlecan of heparan sulfate proteoglycan, and is localized beneath all kinds of epithelial and endothelial cells [13]. Depending on the biological activity of each component, basement membrane has multiple and integrated functions including serving as a scaffold for cells, separating cell compartments, and directing cell proliferation, migration, differentiation, and apoptosis [14]. The composition of

☆ This Study Funded by: A scientific research grant from the Ministry of Education, Culture, Sports, Science and Technology of Japan (14570532 to T.B.).
* Corresponding author. Fax: +81 11 706 7899.
E-mail address: bytomoko@med.hokudai.ac.jp (T. Betsuyaku).

0006-291X/$ - see front matter © 2008 Elsevier Inc. All rights reserved.
doi:10.1016/j.bbrc.2008.01.105

basement membrane varies according to the stage of lung development [15]. For instance, laminin-332 (formerly termed laminin-5 [16]) is ubiquitously present both in embryonic and adult lungs [17], whereas laminin-111 (formerly termed laminin-1 [16]) expression is restricted to the early stage of lung development [15].

We recently developed a novel substratum that mimics basement membrane structure for cell culture, which we termed synthesized basement membrane (sBM) substratum [18]. The sBM substratum is generated using immortalized rat alveolar type II epithelial cells, SV40T2 cells, in the presence of Matrigel®, in which laminin-111 and entactin/nidogen are exogenously supplied by Matrigel® dissolved in the culture medium, while laminin-511 (formerly termed laminin-10 [16]), type IV collagen and heparan sulfate proteoglycan production is endogenously driven by SV40T2 cells [18,19]. We also found that sBM substratum has the capacity to accelerate the growth and differentiation of rat tracheal epithelial (RTE) cells *in vitro* [19]. Recently, sBM substratum was also reported to be useful to efficiently maintain the hepatocyte-associated phenotype in culture [20]. Considering the presence of laminin-111 as a major laminin isoform incorporated in this synthesized substratum, sBM substratum may have similar features to the basement membrane of embryonic lung. Therefore, we hypothesized that sBM substratum may affect the transcriptional regulation of EMMPRIN by airway epithelial cells.

Materials and methods

Culture medium and supplements. The basal medium consisted of an equal volume mixture of Dulbecco's modified Eagle's medium and Ham's F12 medium (DMEM/F12) (Gibco, Carlsbad, CA, USA) containing 100 U/ml penicillin G potassium (Meiji Seika, Tokyo, Japan), and 100 μg/ml streptomycin sulfate (Meiji Seika, Tokyo, Japan). The complete medium formula was basal medium supplemented with 10 μg/ml insulin (Sigma, St. Louis, MO, USA), 0.1 μg/ml hydrocortisone (Sigma), 0.1 μg/ml cholera toxin (List Biological Laboratories, Campbell, CA, USA), 5 μg/ml transferrin (Sigma), 50 μM phosphoethanolamine (Sigma), 80 μM ethanolamine (Sigma), 25 ng/ml epidermal growth factor (Toyobo, Osaka, Japan), 30 μg/ml bovine pituitary extract (Sigma), 0.5 mg/ml bovine serum albumin (Sigma), and fresh 50 nM retinoic acid (Sigma) [19].

Preparation of RTE cells. Experimental protocols and procedures were approved by the Ethics Committee on Animal Research of the Hokkaido University School of Medicine. RTE cells were harvested and cultured as previously described [19]. Briefly, male Sprague–Dawley rats, 8–10 weeks of age (Japan Clea, Tokyo, Japan), were exsanguinated, and the tracheas were removed *en bloc* and filled with 1% Pronase E (Sigma) for overnight incubation at 4 °C. The recovered cells were suspended in DNase I (Roche Diagnostics, Indianapolis, IN, USA) solution, and then re-suspended in complete medium. These freshly isolated primary RTE cells were seeded into the wells of type I collagen coated culture plates (Becton–Dickinson Labware, Franklin Lakes, NJ, USA), and cultured until 80% confluence. We defined those cells as passage zero. These cells were then harvested and re-seeded on type I collagen coated plates and cultured; denoted as the 1st passaged cells. Subsequently, these cells were harvested and re-seeded again on various matrices of basement membrane components. These were denoted as the 2nd passaged cells.

Culture of the 2nd passaged cells on various matrices of basement membrane components. We first used the sBM substratum to assess the induction of EMMPRIN by the 2nd passaged cells. As previously described, sBM substratum was prepared [18,19]. Other coated plates were prepared as follows: mouse laminin-111 (Becton–Dickinson Labware) and rat laminin-332 (Chemicon, Temecula, CA, USA) were coated on six-well plates (Becton–Dickinson Labware) at concentrations of 10 μg/ml and 1 μg/ml, respectively, for 24 h at 37 °C, and bovine type IV collagen (Nitta Gelatin, Osaka, Japan) was coated on six-well plates (Becton–Dickinson Labware) at a concentration of 100 μg/ml in 1 mM hydrochloric acid at room temperature until air-dried. The 2nd passaged cells were seeded on each substratum at a density of 1.5–2.0 × 10^5 cells/cm^2, and then cultured at 37 °C in 5% CO_2. Non-adherent cells were removed after 6 h. The remaining cells were cultured until analysis at each time point indicated.

Quantitative reverse transcriptase-polymerase chain reaction. Total RNA was extracted from cultured cells using the SV Total RNA Isolation kit (Promega, Madison, WI, USA). After reverse transcription, 5′-exonuclease-based fluorogenic PCR was performed using an ABI PRISM 7700 Sequence Detector (PE Applied Biosystems, Foster City, CA, USA). Primers and a labeled probe for EMMPRIN (Assay ID Rn00562874_m1), MMP-9 (Rn00579162_m1), transforming growth factor-α (TGF-α) (Rn00562037_m1), epidermal growth factor (EGF) (Rn00563336_m1) and β2-microgloblin (β2-MG) (Rn00560865_m1) were purchased from PE Applied Biosystems. The relative amount of mRNA in the samples was normalized against β2-MG mRNA.

Gelatin zymography. Gelatinolytic activity in conditioned medium was assessed by gelatin zymography as described [21]. Conditioned medium was concentrated 10-fold using a Millipore Ultrafree system (Millipore, Tokyo, Japan). Sodium dodecyl sulfate (SDS)–polyacrylamide gel electrophoresis was performed under non-reducing conditions using a 10% (w/v) separating gel containing 1 mg/ml gelatin. Pro-MMP-9 standard sample derived from human fibrosarcoma cell line (Wako, Osaka, Japan) was applied concurrently. After electrophoresis, the gel was shaken gently in 2.5% Triton X-100 at room temperature for 30 min to remove SDS, and

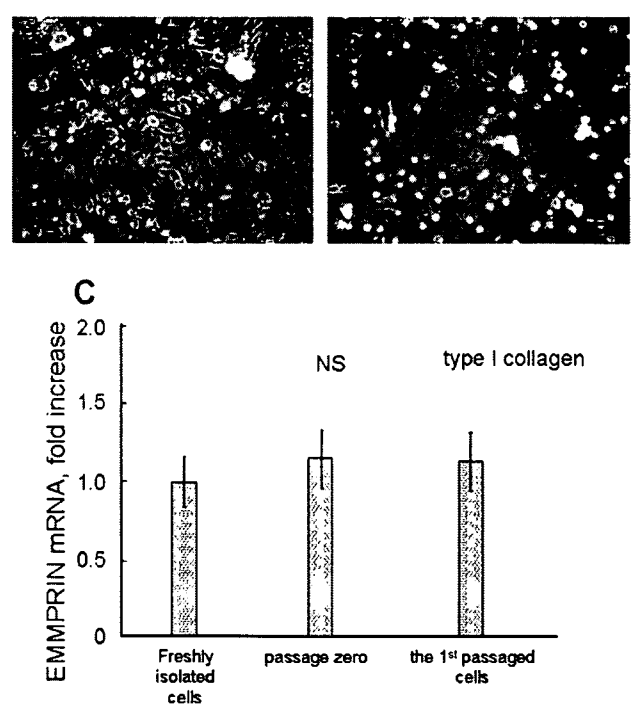

Fig. 1. Phase contrast microscopic appearance of passage zero (A) and the 1st passaged (B) cells. EMMPRIN mRNA levels in RTE cells during passage on type I collagen (C). "Fold increase" refers to EMMPRIN mRNA levels detected under each condition compared to the freshly isolated cells. Bar = 50 μm.

then incubated in reaction buffer (0.2 M NaCl, 5 mM $CaCl_2$, 1 μM $ZnCl_2$, 50 mM Tris–HCl, pH 7.6) at 37 °C for 18 h. The gels were stained with 0.25% Coomassie brilliant blue R-250 and destained. The enzyme activity was then detected as a clear band on the resulting blue background of undigested gelatin.

Immunocytofluorescence for EMMPRIN. For immunofluorescent analysis, the 2nd passaged cells cultured on laminin-111 were fixed in 4% paraformaldehyde (30 min). Cells were incubated with the anti-rat EMMPRIN monoclonal antibody (clone MRC OX-47, Serotec, Oxford, UK) at 1:200 dilution followed by a secondary antibody fluorescein-5-isothiocyanate (FITC)-conjugated goat affinity purified antibody at 1:100 dilution (MP Biomedicals, Irvine, CA). The resulting fluorescence was observed with a Leica DMRBE microscope.

Statistical analysis. Data are expressed as means ± standard error (SE). Statistical analysis was performed with single factor analysis of variance followed by Fisher's protected least significant difference using SAS program release version 8.2 for Windows XP or the StatView J 5.0 System (SAS Institute Inc., Cary, NC). $p < 0.05$ was considered statistically significant.

Results

EMMPRIN expression during subculture on type I collagen

To examine whether the expression of EMMPRIN is altered during subculture on type I collagen, primary RTE cells were cultured for two passages as described previously [19]. Although the RTE cells initially had polygonal and cobble stone shapes during the 3–4 days of culture during passage zero (Fig. 1A), the number of cells with multi nuclei increased before the 2nd passage (Fig. 1B), indicating accelerated proliferation between the 1st and 2nd passage. Following the two passages, ciliated cells had almost disappeared. In spite of the dramatic phenotypic changes, there was no change in the level of EMMPRIN mRNA in the RTE cells subcultured on type I collagen (Fig. 1C).

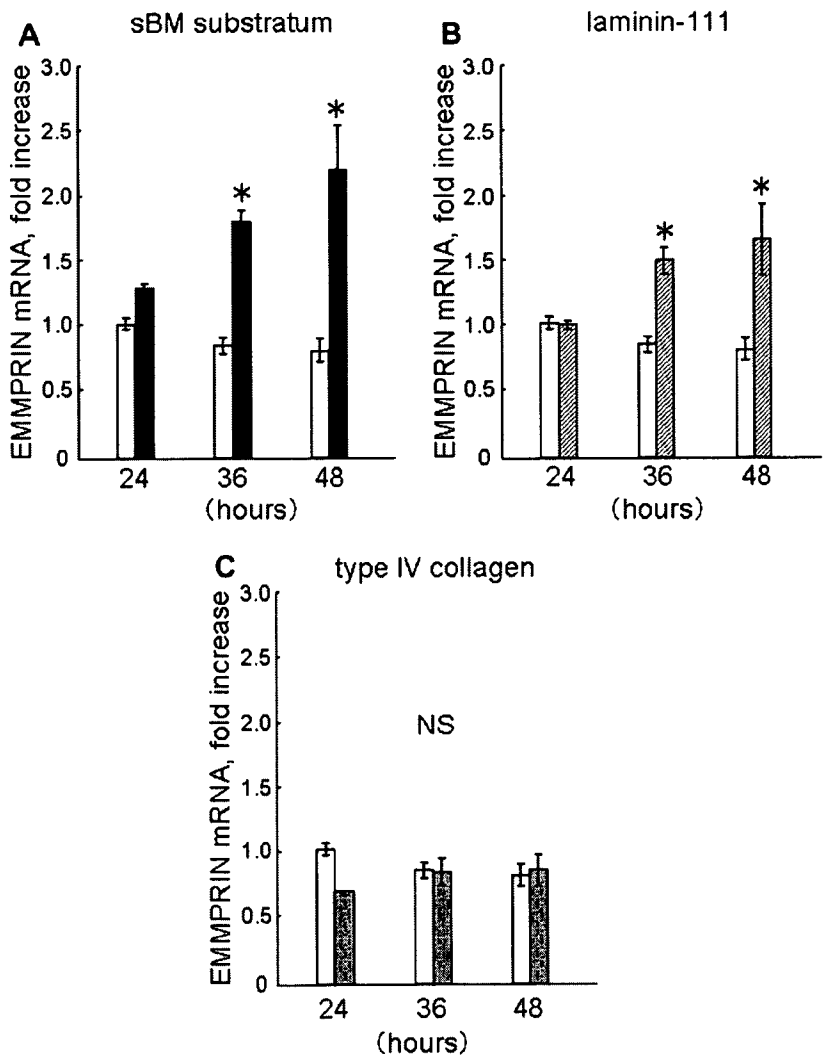

Fig. 2. Expression of EMMPRIN on sBM substratum, laminin-111, and type IV collagen. The 2nd passaged cells were cultured on either sBM substratum (black bars) (A), laminin-111 (hatched bars) (B), type IV collagen (shaded bars) (C), or plastic (white bars) for 24, 36, or 48 h. "Fold increase" refers to EMMPRIN mRNA levels detected under each condition at the indicated time points compared to those in culture on plastic for 24 h. $^*p < 0.05$ vs. plastic at each time point.